

# Microsystems for Drug and Gene Delivery

MICHAEL L. REED, SENIOR MEMBER, IEEE AND WHY-KEI LYE, MEMBER, IEEE

## Invited Paper

*Microneedles and other structures have been developed for introducing therapeutic agents into tissues and cells. Microstructures for transdermal delivery hold the promise of pain-free drug injection. Electrodes integrated with microneedles can sense and monitor the effects of injected materials on tissues. Microprobes have been shown to be effective in transfecting cells through the delivery of DNA in experiments with both plants and animals. Microfabricated delivery devices have great potential for local delivery of drugs and genes where systemic administration presents serious safety concerns. In this paper, we review recent progress in microdevices for delivering therapeutic agents, including microneedles, DNA transfection schemes, and intravascular drug and gene delivery systems.*

**Keywords**—Drug delivery systems, gene delivery, microfabrication, micromachining, microneedles, microsystems, restenosis, stent.

## I. INTRODUCTION

Application of microfabrication technologies developed for electronic integrated circuits in the biomedical area has been largely directed toward diagnostics, such as microfabricated pressure transducers, thermometers, ultrasonic sensors, and the like. More recently, there has been considerable activity in “lab-on-a-chip” applications where a large number of chemical or biological assays are performed in parallel. Gaining in importance are applications of microsystems technology to therapeutics, where microfabricated devices are used to treat diseases rather than diagnose them.

In this paper, we discuss the use of microfabrication technology applied to microsystems for drug and gene delivery, with an emphasis on the process technology for manufacturing the delivery device. We first review various technologies developed for fabricating microneedles capable of piercing the skin or other tissues. Next, we discuss microprobe structures which have been used to transfer

DNA into cells as an alternative to microinjection, cell bombardment, electroporation, adenoviruses, and liposome delivery methods. We conclude with the development of a microsystem for mechanically transporting drugs or genes into the vascular system, which will be especially useful for delivering anti-restenosis therapies following balloon angioplasty.

Many of the devices discussed in the referenced articles, particularly microfabricated needles, are designed for transdermal therapies—to painlessly deliver a bolus into subcutaneous tissue whereupon it is distributed systemically by the circulation. This is necessary for some drugs (insulin, heparin, etc.), but not ideal for others (such as anti-restenosis and anti-tumor therapies). Microneedles and other microfabricated devices can also be adapted for *local delivery*. (The idea is that therapeutic agents designed to reach a particular area where disease is progressing (for example, in a blocked coronary artery or a localized tumor) can be administered systemically through the bloodstream, but this results in a decreased dose at the needed site, since the agent is diluted by the entire blood volume.) Achieving a clinically relevant dose can often lead to side effects, including toxicity, when drugs are delivered in this way. In contrast, local delivery concentrates the agent where it is needed; thus, a lower, generally safer total dose can be administered, and side effects encountered with systemic delivery are avoided. Microsystems technology has the potential to radically improve the range of applications for local delivery by the creation of new delivery platforms, which will in turn enable the development of new therapies.

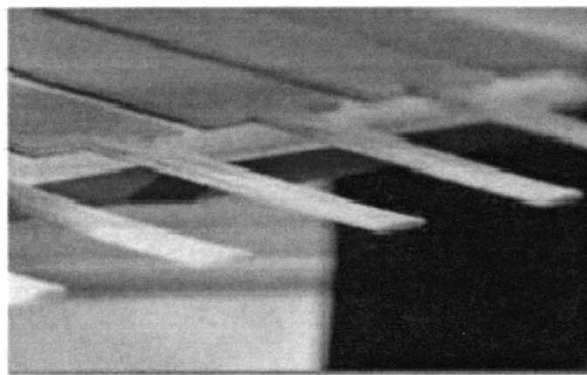
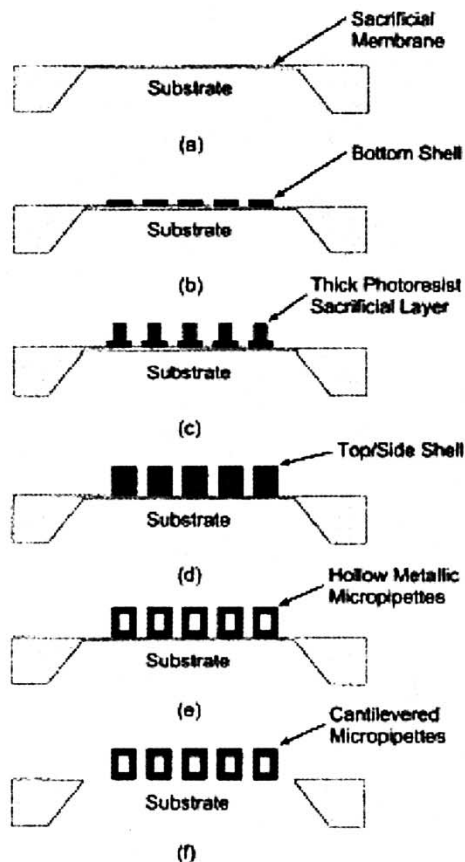
## II. MICRONEEDLES

Hollow needles terminating in a sharp point, mounted at the end of a syringe, are familiar to all. Microfabricated needles have been developed in several materials: silicon, glass, and metal. Microneedles can be fabricated in-plane, where the needle lumen (flow channel) is parallel to the substrate surface, or out-of-plane, where the lumen is normal to the substrate. They can be used to deliver agents through the skin,

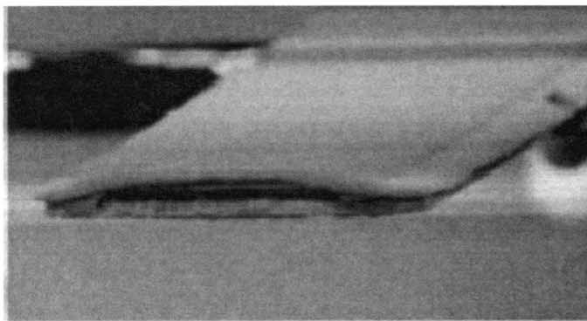
Manuscript received March 30, 2003; revised July 13, 2003. This work was supported in part by Setagon, Inc.

The authors are with the Department of Electrical and Computer Engineering, University of Virginia, Charlottesville, VA 22904-4743 USA (e-mail: reed@virginia.edu; wklye@virginia.edu).

Digital Object Identifier 10.1109/JPROC.2003.820542



(a)



(b)

**Fig. 1.** Fabrication process and micrographs of hollow in-plane metal microneedles fabricated by electroforming (Papautsky *et al.* [5]).

into a blood vessel, or into a cell, or can extract fluids by reversing the flow direction. They can be integrated with microelectrodes to gauge the cellular response to agents in real time. Microneedles must cleanly pierce the tissue without plugging the lumen.

Microfabricated microneedles are the subject of an extensive review paper [1] by McAllister *et al.*, published in 2000. In the discussion below, we include advances in microneedle fabrication which have been reported since the publication of this paper. The technologies are grouped with in-plane microstructures first, out-of-plane devices second.

### A. In-Plane Microneedles

In-plane microstructures, where the shaft and lumen are parallel to the substrate surface, have their long dimension defined lithographically. It is, thus, straightforward to control their length. This advantage is offset by the restriction to one-dimensional (1-D) arrays, and the need to remove substrate material beneath the microneedles to create isolated structures. In-plane microneedles formed by thin-film deposition can be quite fragile. This problem can be overcome by retaining some of the underlying silicon substrate near the microneedle to add structural strength.

Brazzle *et al.* [2]–[4] and Papautsky *et al.* [5] have fabricated arrays of in-plane metal microneedles useful for drug delivery, fluid extraction, and reagent delivery in chemical

microinstruments, using a micromolding process. The fabrication process, shown in Fig. 1, begins with the formation of a P+ etch stop layer and backside anisotropic etching in KOH to define a thin membrane. The lower wall of the microneedle consists of deposited and patterned metal layers. A thick layer (5–50  $\mu\text{m}$ ) of positive photoresist is then spin coated and lithographically patterned on top of the lower metal walls. The dimensions of this sacrificial layer precisely define the cross section of the lumen. After sputter deposition of a Pd seed layer, the thick metal structural walls and top of the microneedles are formed by electrodeposition. The sacrificial photoresist is removed with acetone, and the P+ membrane etched away in an SF<sub>6</sub> plasma, resulting in a 1-D array of hollow microneedles released from the substrate.

Typical lateral dimensions of the microneedles designed to penetrate into skin range from 10 to 1000  $\mu\text{m}$ ; lengths range from 50  $\mu\text{m}$  to a few millimeters. These dimensions are dictated by the need to penetrate through the stratum corneum (10–15  $\mu\text{m}$  of dead tissue), and the epidermis (50–100  $\mu\text{m}$  of live cells, but without blood vessels and few nerve endings) into the dermis, where the network of blood vessels resides. The dermis also contains most of the nerves, so by minimizing the penetration depth into this layer, the pain associated with insertion can also be minimized.

The mechanical behavior of microneedles fabricated using this process has recently been reported by Chandrasekaran and Frazier [6], [7] (Fig. 2). Time-dependent

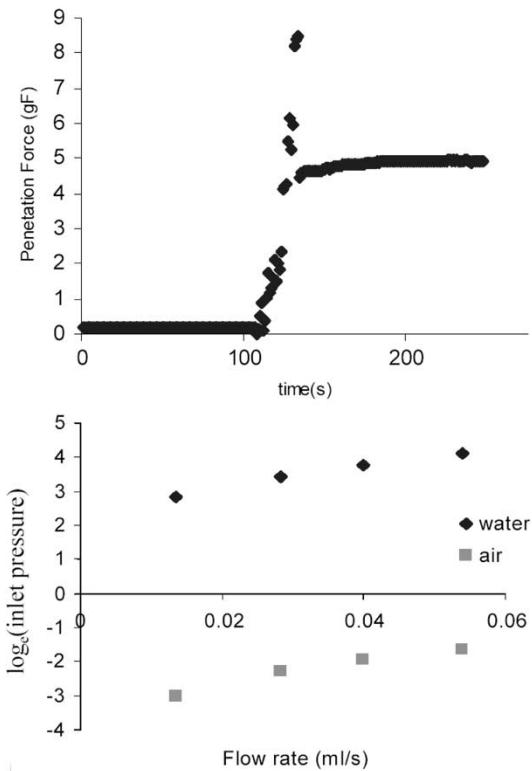
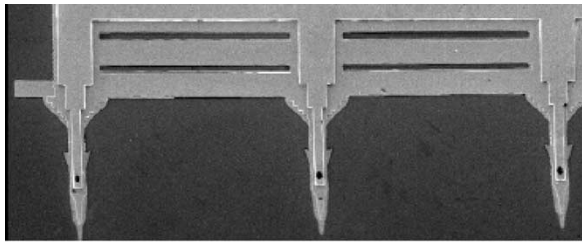


**Fig. 2.** Mechanical behavior of in-plane microneedles tested by Chandrasekaran and Frazier [6], [7]. Top: micrograph of needle arrays. Center: needle force versus time during penetration test. Bottom: volumetric flow rate for various pressures.

penetration force (center of figure) was measured by forcing the needle against a skin-like material (photoelastic sheet PS-4B). The peak force is approximately 8.5 grams force for a 1.5-mm-long needle. This force is approximately one-tenth of that required to buckle the needles, as tested by pressing the microneedles against a rigid surface. The flow characteristics of 1-mm-long needles (bottom graph) show that pressures of 49 to 243 Pa result in flow rates of 0.014 to 0.068 ml/s for air; for water, pressures of 3.0 to 12.1 kPa are required to produce flow rates of 0.017 to 0.67 ml/s.

Lin and Pisano [8] have fabricated microneedles for fluid delivery and neuronal monitoring in a silicon-based process (Fig. 3). The primary structural material of these microneedles is silicon nitride, forming the top, and a bulk micromachined boron doped silicon boss defined by etching the substrate in ethylene-diamine pyrocatechol (EDP). This layer of silicon, which varies in thickness from about 50  $\mu\text{m}$  at the shank to 12  $\mu\text{m}$  near the tip improves the structural strength. The lumen is defined by a sacrificial layer of phosphorus doped glass.

These microneedles are 1–6 mm in length with lumens 9  $\mu\text{m}$  high and 30 or 50  $\mu\text{m}$  wide. The proximal ends of the microstructures have integrated polycrystalline silicon heater strips. These heaters can generate bubbles, which are useful in pumping fluid down the lumen. Also, electrodes can be patterned along the length of the needle by a slight process modification; these are useful for measurements of neural activity. The authors report that their needles (70- $\mu\text{m}$  height, 80- $\mu\text{m}$  width) have repeatedly penetrated animal tissue (porterhouse steak) without bending or breakage.

A different approach to fabricating an in-plane integrated fluid delivery/microelectrode needle structure was developed by Chen *et al.* [9] (Fig. 4). The flow channel is recessed into the silicon substrate, defined by a novel process using an array of chevron-shaped P+ silicon masks and anisotropic etching in EDP. This process uses the differential etch rates characteristic of the crystallographic planes in silicon to define the channel dimensions, which results in extremely tight dimensional control. The authors report the ability to fabricate arrays of channels with a channel-to-channel spacing of as little as 4  $\mu\text{m}$ . After the EDP etch, the recessed channel is sealed by oxidizing the chevrons (volumetric expansion during oxidation causes the spaces to close up) followed by low pressure chemical vapor deposition (LPCVD) of a dielectric. The process can be used for channels from 10  $\mu\text{m}$  to 100  $\mu\text{m}$  wide. Below 10  $\mu\text{m}$ , the channel sealing process blocks the channels; above 100  $\mu\text{m}$ , changes are necessary to the mask to correct for strain and stress effects. (Also, only 90° turns in the fluid channel are possible.) The resulting surface is planarized by dry etching to accommodate metal microelectrodes placed along the length of the shaft. The remainder of the needle structure is defined by a P+ etch stop layer and bulk micromachining.

Microneedles produced with this process have widths of 58 to 74  $\mu\text{m}$ , and are 4 mm long. The lumen is approximately 15  $\mu\text{m}$  deep and 10 to 32  $\mu\text{m}$  wide.

The fabrication process for these microneedles is fully CMOS compatible. The shank end contains microelectronic circuitry for sensing the signals produced by cells in contact with the microelectrodes. The probes have been used for monitoring the neural responses to various chemical stimuli delivered through the microneedle lumens *in vivo* in guinea pigs.

The preceding processes all result in in-plane microneedles attached to a silicon substrate. Detached microneedles have been fabricated with a polysilicon molding process by Talbot and Pisano [10] (Fig. 5). The two halves of the mold are produced by bulk micromachining of silicon wafers followed by deposition of a 2- $\mu\text{m}$  phosphosilicate glass (PSG) release layer. The two halves are temporarily bonded together under nitrogen pressure at 1000 °C. After bonding, a 3- $\mu\text{m}$  layer of amorphous silicon is deposited by LPCVD through access holes in the top mold wafer. The LPCVD process produces highly conformal coatings with a uniform thickness. The mold (and deposited film) is then annealed at 1000 °C in nitrogen. Deposition and annealing steps are repeated until the desired thickness (typically 12 to 18  $\mu\text{m}$ ) is obtained. Anisotropic plasma etching is used to remove the polysilicon

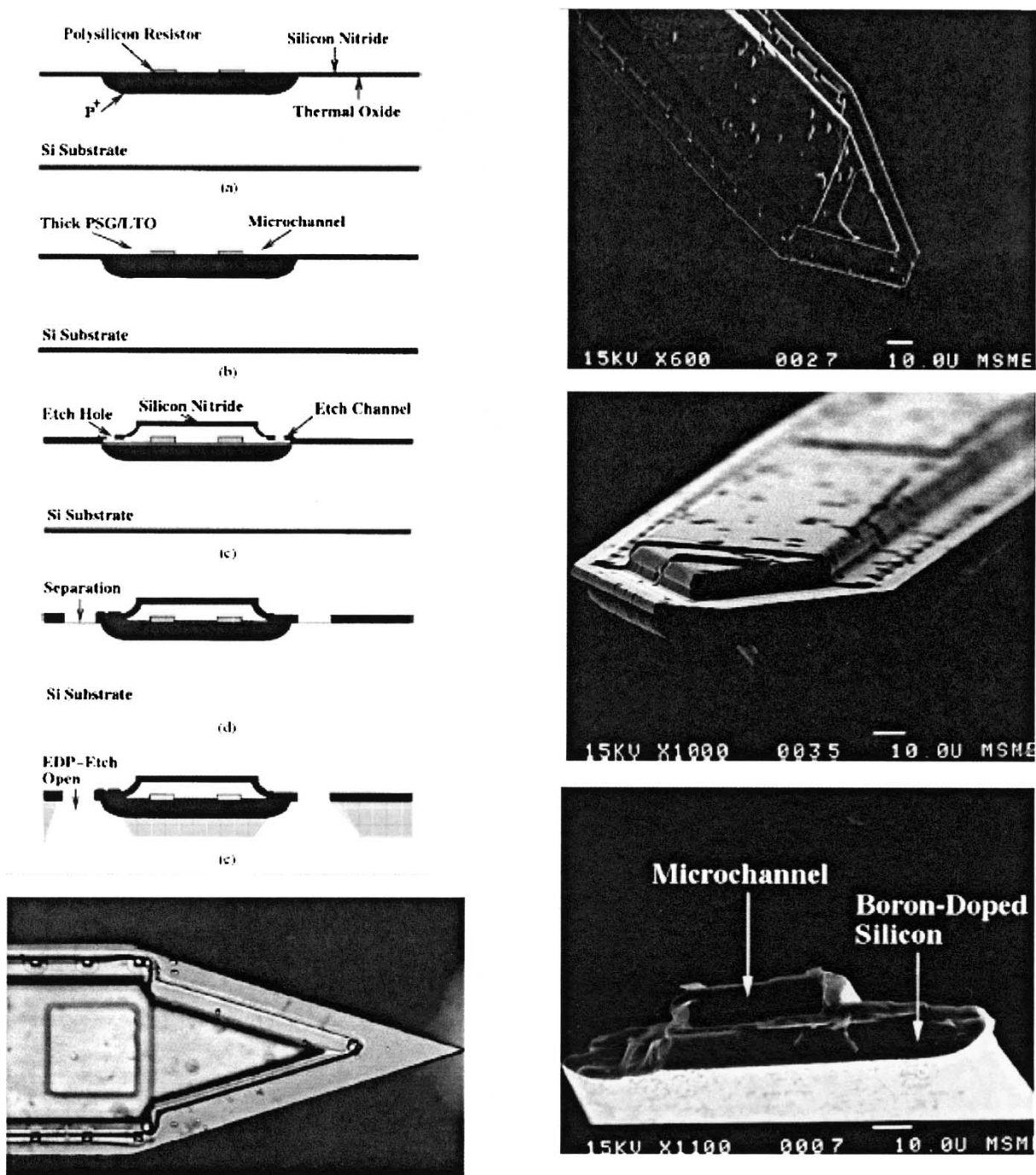
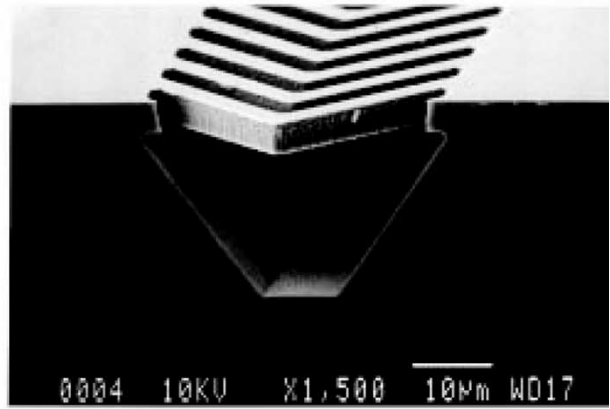
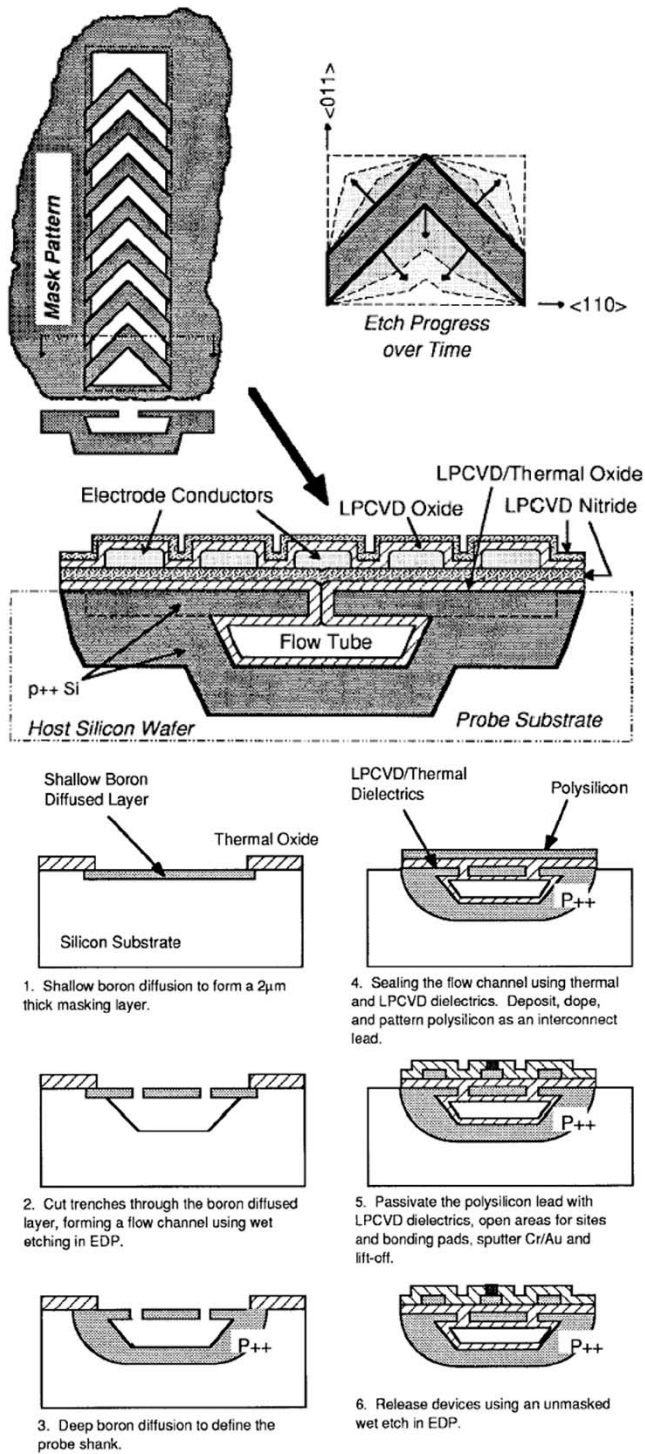


Fig. 3. In-plane microneedles developed by Lin and Pisano [8].

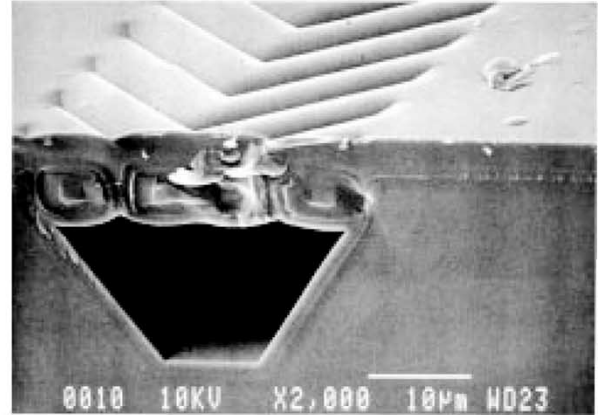
coating the funnel-shaped access holes in the top mold layer. The devices are released from the mold by extended etching in concentrated hydrofluoric acid which selectively attacks the PSG. The molds can be used repeatedly by redepositing the release layer, which helps to reduce manufacturing cost.

The resulting polysilicon microneedles are 1 to 7 mm long, with 110- by 200- $\mu\text{m}$  rectangular cross sections, and sub-micrometer tip radii. The devices could withstand bending moments of 0.53 mN-m. The mechanical strength can be increased (up to 0.71 mN-m) by sputtering or plating Ni on the finished structures.

Microneedles fabricated using this polysilicon molding process have been incorporated into microfluidic systems by Zahn *et al.* [11]–[13]. An electron micrograph of a microneedle mold and the resulting artifact is shown in Fig. 6, taken from [11]. In this paper they describe a micromolding fabrication process substantially similar to Talbot [10], but employing a single double-polished silicon wafer instead to a bonded sandwich mold. This improvement eliminates the tedious alignment step required when bonding the two wafers together. Zahn *et al.* [14] have also integrated diffusion structures for separating species by molecular



(a)



(b)

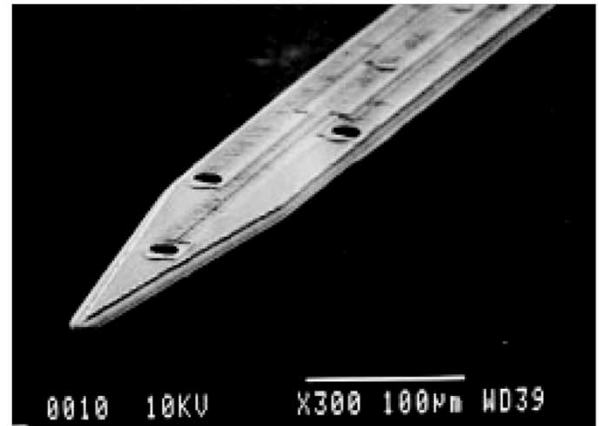
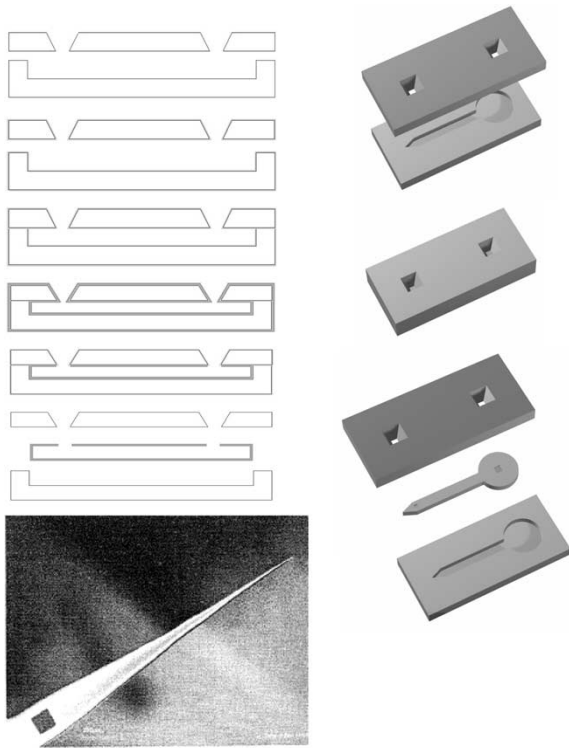


Fig. 4. In-plane microneedles with integrated electrodes and a buried flow channel (Chen *et al.* [9]).

weight with microneedles fabricated using a surface micro-machining process for microdialysis applications.

A highly jagged microneedle device for trace blood collection was developed by Oka *et al.* [15] (Fig. 7). The structure mimics the shape of a mosquito proboscis and is integrated with a reservoir for holding the extracted blood. The jagged edge is said to increase the ease of penetration through the skin and reduce the contact area with the dermis. The key

steps in producing the jagged geometry rely on the formation of the negative pattern by anisotropic etching of silicon. The slow-etching  $\langle 111 \rangle$  planes meet at well-defined angles, forming a saw-like edge in cross section. By varying the pattern spacing, the depth of the V-shaped grooves in the silicon decreases toward the tip, resulting in an in-plane microstructure with a nonuniform depth. The structural material of the needle is  $\text{SiO}_2$  formed by thermal oxidation after



**Fig. 5.** Microneedles fabricated from a polysilicon molding process using two silicon wafers (Talbot and Pisano [10]).

bonding with a second wafer. The excess silicon around the needle is removed by plasma etching and the needle reinforced by deposition of  $1\ \mu\text{m}$  of polysilicon. The hole connecting the lumen to the outside is cut by a focused ion beam. Microneedles have been tested for penetration through silicon rubber, and collection of ink through an external pump has been demonstrated.

### B. Out-of-Plane Microneedles

Out-of-plane microneedles have their lumen and long dimension perpendicular to the wafer substrate. This makes it possible to control the lumen and lateral shaft dimensions lithographically in both planes orthogonal to the shaft length. In contrast, in-plane microneedles generally have one of these dimensions controlled by a film or doped layer thickness, which is impractical to increase beyond a few micrometers or tens of micrometers. Out-of-plane microneedles can, thus, be very robust. They can also be fabricated in two-dimensional arrays with macroscopic dimensions, increasing their volumetric flow capability. The chief disadvantage of out-of-plane structures is that the long dimension is not defined lithographically but often by a removal process, which can be costly, time consuming, and difficult to control. Fluid access to the microneedle lumens is through the backside of the wafer, necessitating two-sided wafer alignment capability or wafer bonding, adding complexity to the process. Out-of-plane manufacturing methods are also more difficult to integrate with electronic processes, owing to the short depth of focus of lithographic alignment tools.

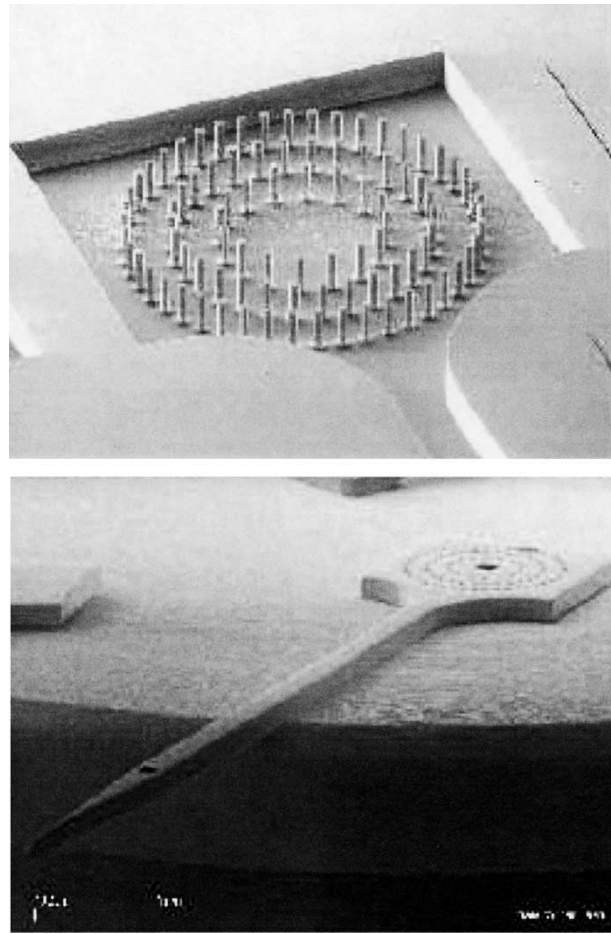


**Fig. 6.** Planar microneedles fabricated by Zahn *et al.* [11] using the micromolding process.

Stoerber and Liepmann have fabricated out-of-plane microneedles [16], [17] (Fig. 8) and incorporated arrays of their structures into a microfabricated syringe [18]. The fabrication process starts with oxidized double-sided polished silicon wafers. The lumen is etched through the wafer by deep reactive ion etching following a mask patterned on the wafer backside. A silicon nitride film is deposited across the backside and into the etched hole, protecting the lumen from the etch step performed later in the process. Needle locations are defined lithographically in a masking film on the top of the wafer. The microneedle shafts are created by isotropic etching of the silicon substrate. For long etch times, the radius of curvature of the silicon near the mask edge becomes large, forming a microneedle with a gradually increasing diameter along the shaft. By displacing the circular isotropic etch mask from the center of the lumen (dimension  $\delta$  in Fig. 8), a pointed needle shape is obtained.

These microneedles, designed for painless transdermal delivery, are  $200\ \mu\text{m}$  tall, with a base diameter of  $425\ \mu\text{m}$  tapering to a  $40\text{-}\mu\text{m}$  lumen. Individual needles are spaced  $750\ \mu\text{m}$  apart. Fluid injection was demonstrated by delivering ink under the skin of a chicken thigh, a depth of approximately  $100\ \mu\text{m}$ . The syringe microsystem incorporated a  $20\text{-}\mu\text{l}$  reservoir on the back of the microneedle array and

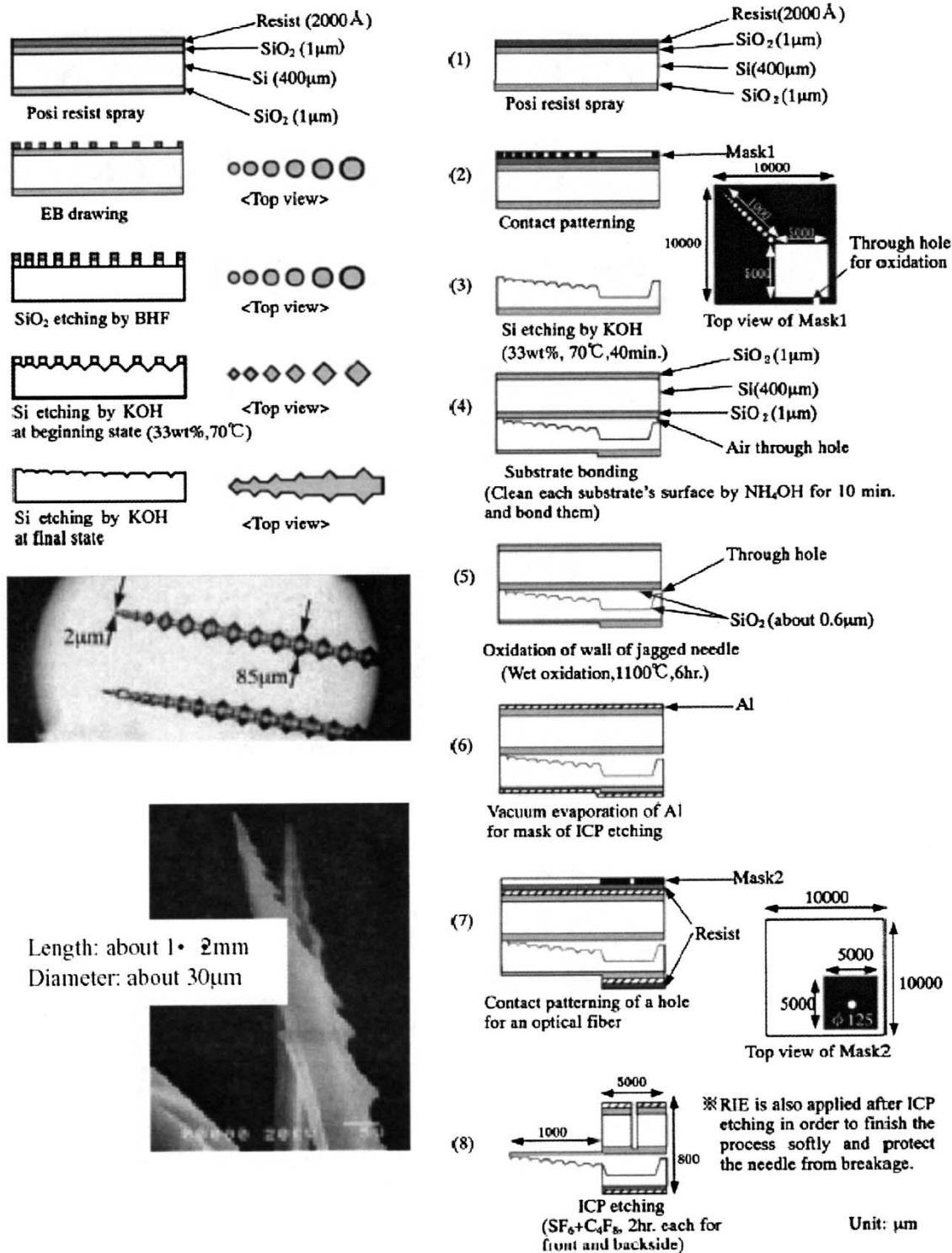
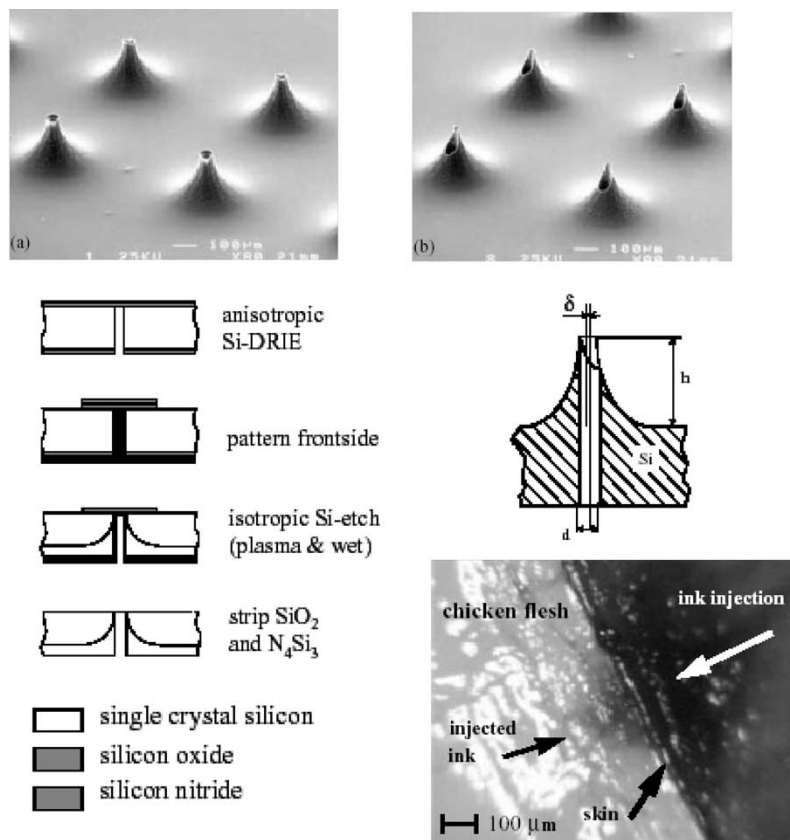


Fig. 7. Jagged microneedles for trace blood collection developed by Oka *et al.* [15]. The device is modeled after a mosquito proboscis, shown in the photograph in the lower left.

successfully injected aqueous suspensions of 0.7- $\mu\text{m}$ -diameter polystyrene beads. None of the structures broke during the testing; it is likely that the short squat geometry of these microneedles helps to prevent breakage when they are subjected to lateral forces.

Solid silicon microneedles with no lumen have been developed for transdermal drug delivery by Henry *et al.*

[19]–[20] (Fig. 9). The fabrication process is simple, employing a chrome mask combined with deep reactive ion etching in a process originally designed to produce scanning probe microscope tips [21]. Etching proceeds until the mask falls off from underetching. The needle taper is controlled by adjusting the degree of anisotropy in the etch process. The resulting microneedles are 150  $\mu\text{m}$  tall and can be fabricated



**Fig. 8.** Out-of-plane single crystal silicon microneedles developed by Stoeber and Liepmann [17]. Top: symmetric and asymmetric needles, about  $200\ \mu\text{m}$  high, with lumen diameters of  $40\ \mu\text{m}$ . Center: simplified fabrication process, starting with double-sided polished silicon wafers. The drawing at center right illustrates how a sharp tip is produced by displacing the centerline of the microneedle and lumen by an amount  $\delta$ . Bottom right: demonstration of blue ink injected into a chicken thigh.

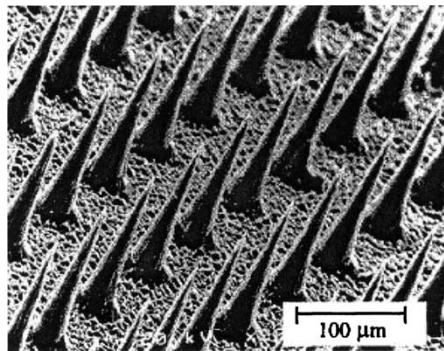


**Fig. 9.** Solid silicon microneedles with no lumen fabricated by reactive ion etching [19].

in dense arrays. Since they have no lumens, they are not used as a conventional hypodermic needle. Rather, they are designed to increase the skin permeability as a means of enhancing drug diffusion. Holes left by the array are approximately  $1\ \mu\text{m}$  across, and were observed to increase permeability by a factor of 1000 to 25 000 depending on the amount of time they remained embedded in the skin. Despite their seeming fragility, these microneedles were quite robust and only a small number broke during testing.

Separating the functions of tissue penetration and fluid delivery is relatively straightforward for in-plane microneedle designs, where the tip shape and fluid openings are defined

lithographically. It is considerably less straightforward for out-of-plane designs, where the tip is an annulus whose inner surface is the microneedle lumen. An out-of-plane microneedle with separate penetration and delivery structures was successfully demonstrated by Griss and Stemme [22], [23] (Fig. 10). The idea is to have a very sharp tip for ease of penetration, but without an annulus typically found in a microneedle, which can result in plugging of the lumen. Instead of a delivery channel at the end, the liquid flows through openings in the side of the microneedle.

The key step in the fabrication process is illustrated. A series of masking, backside reactive ion etch, and frontside reactive ion etch steps produce the structure shown at the bottom left of Fig. 10. The opening in the center has a circular cross section formed by a backside etch, while the  $\text{SiO}_2$  mask on the top is in the shape of a Greek cross. Isotropic plasma etching creates uniform undercutting of this mask. Further isotropic etching reduces the overall dimensions of the structure until the oxidized sidewalls of the lumen are reached. Simultaneously, the silicon pillars under the cross arms of the mask are sharpened to knife edges by the intersection of the isotropic etch fronts. The etch is stopped before the  $\text{SiO}_2$  masking layer falls off. Instead, this layer is removed with a wet chemical etch, which also removes the oxide sidewalls, creating the side openings. A penetrating tip structure is created by subsequent oxidation sharpening. Variations of the

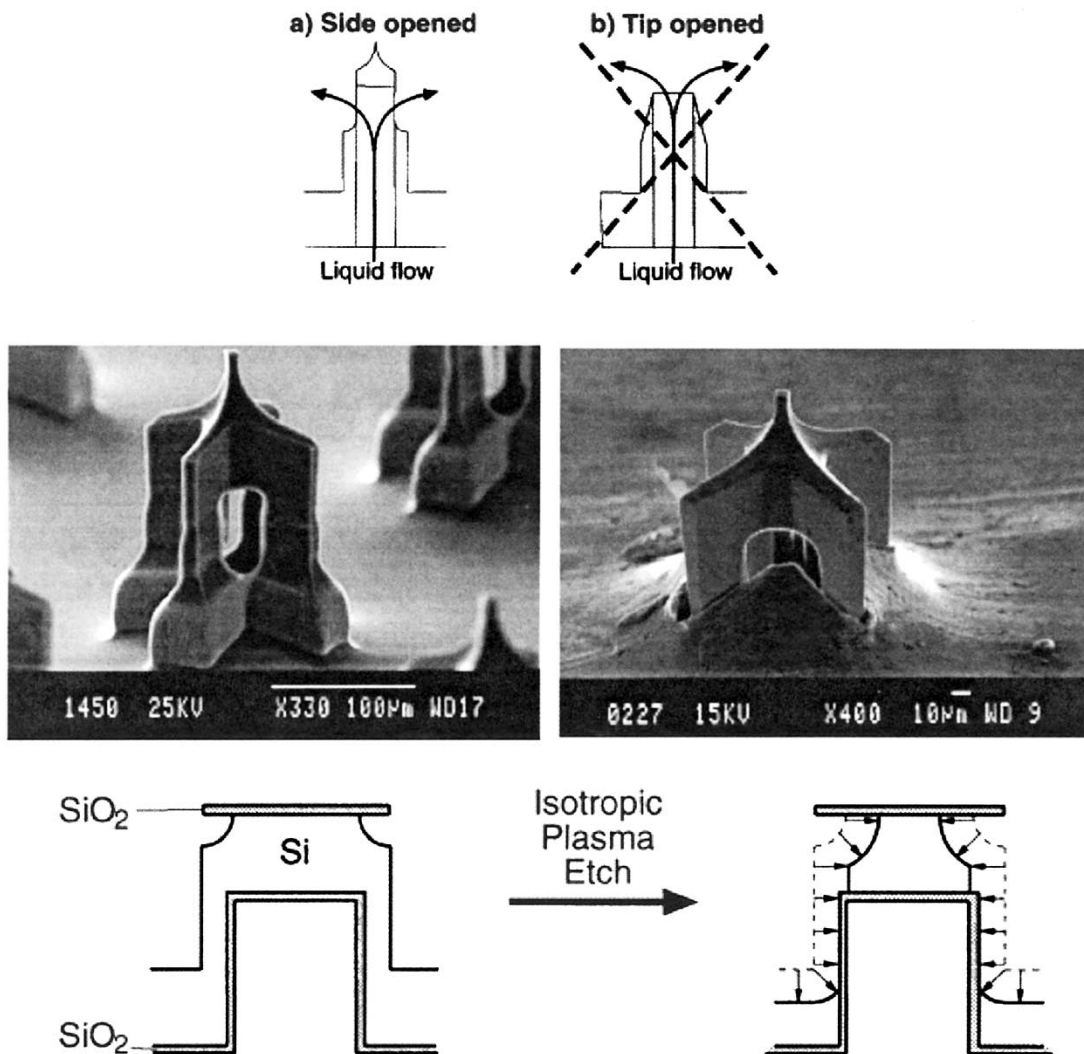


**Fig. 10.** Side-opening out-of-plane microneedles fabricated by Griss *et al.* [22]–[23] Top: positioning of the fluid delivery openings along the side, rather than top, prevents lumen blockage by tissue plugging during penetration. Center: microstructures fabricated by silicon reactive ion etching and related processes. Bottom: the key fabrication step is an isotropic plasma etch, which reduces the overall diameter of the structure.

process make it possible to create side openings which extend completely or only partially along the vertical length of the microneedle.

Microneedles of heights ranging from 100 to 200  $\mu\text{m}$  have been fabricated using this process. The open structure along the side creates a large area for fluid to flow, increasing the area available for exposure to drug compared to a microneedle with an opening at the tip. This feature also presents less resistance to flow. The structures are quite robust; Fig. 10 shows a microneedle penetrating through a 10- $\mu\text{m}$ -thick layer of aluminum foil. The authors report that arrays of these side-opening microneedles can be pressed into human skin repeatedly without breaking and without any associated pain.

Measurements of pressure drop as a function of flow rate for an array of 21 of these side-opening microneedles are shown in Fig. 11. The results are consistent with theoretical calculations (dotted line) assuming Poiseuille flow inside a circular tube [23]. The authors estimate that in a typical trans-

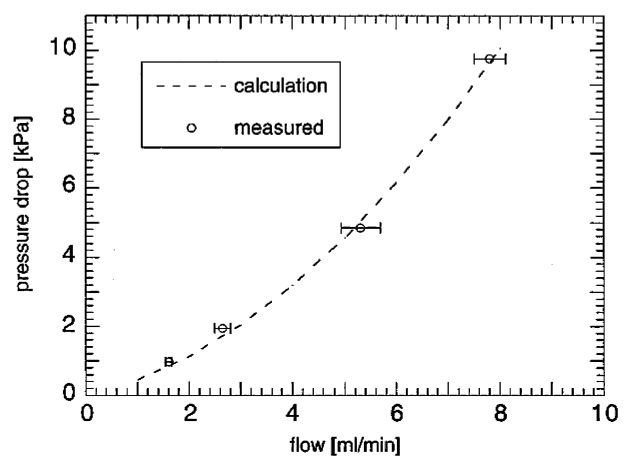


**Fig. 11.** Pressure drop versus flow rate through arrays of the side-opening microneedles fabricated by Griss *et al.* [23].

dermal application such as vaccine delivery, a 100- $\mu\text{l}$  volume of fluid injected through this array over a period of 2 s would

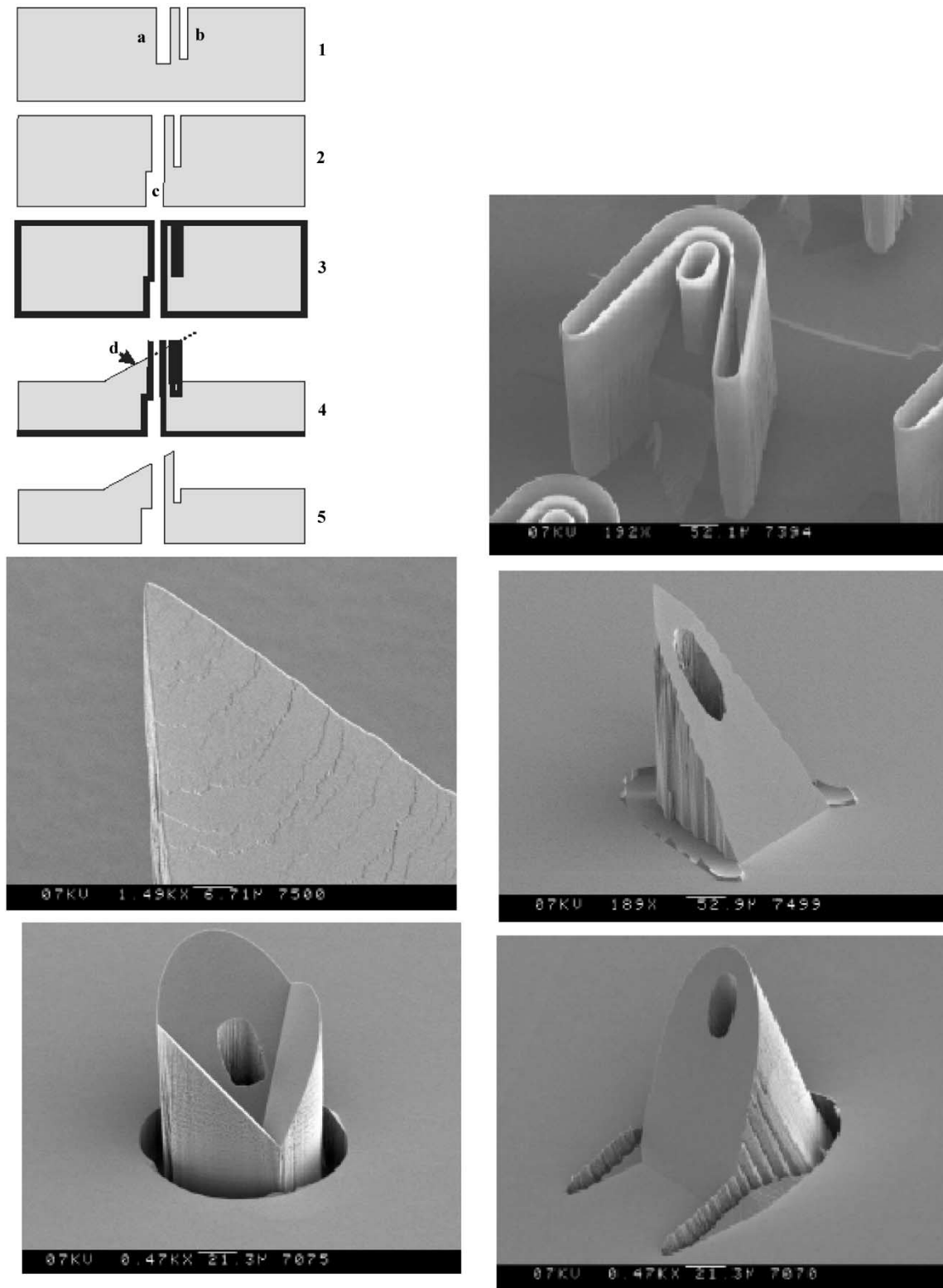


**Fig. 12.** Out-of-plane microneedles fabricated by Gardeniers *et al.* [24]

experience a pressure drop of less than 2 kPa. This flow resistance could be decreased further by increasing the density of out-of-plane microneedles.

Dense arrays of out-of-plane microneedles have been fabricated by Gardeniers *et al.* [24] using an interesting

micromachining process (Fig. 12). The process employs reactive ion etching from both sides of a (100) oriented silicon wafer. A hole (feature “a” in Fig. 12) which will become the lumen and a slot (feature “b”) which defines the position of the needle tip and needle sidewalls are

etched from the front. These structures are aligned to the crystallographic planes of the silicon so that anisotropic etching performed later produces the slanted structure. The connecting lumen (“c”) for fluid delivery is etched from the back. The substrate is then coated with a conformal layer of chemically vapor deposited silicon nitride, including the sidewalls of the etched features. The nitride is removed from the top surface only of the wafer. The nitride acts as a mask during the next step, an anisotropic etch in KOH. This etch leaves a structure defined by the slowest etching (111) plane in the areas where the nitride slot walls are concave, but where the mask is convex, the etch finds all of the fast-etching planes. After removal of the nitride, the microneedle structures are complete.

An important feature of this design is the sharpness of the tip. The leading edge of the microneedle has an extremely sharp radius of curvature, resulting in excellent cutting properties. The location of the opening can be positioned independently of the needle tip, which helps to avoid plugging of the lumen. The flow channel extends all the way through the substrate, leaving space for microfluidic plumbing away from the delivery point, which permits a high density of microneedles to be arrayed over the substrate. Alignment of the needle opening to the tip is performed in a single lithographic step, so complicated backside alignment is not critical in positioning the lumen.

The microstructures shown in Fig. 12 are approximately  $400\ \mu\text{m}$  high, with a base dimension of  $250\ \mu\text{m}$ . Various needle geometries are possible by varying the lithographic design of the slot shape; shown are versions with a curved outer perimeter, and a gouge-shaped microstructure. Arrays of these microneedles have been shown to draw blood through capillary action when pressed into human skin, with no needle failure observed during puncture or withdrawal.

A micromolding process for fabricating biodegradable out-of-plane microneedles has been developed by Park *et al.* [25] The process employs lithographic pattern transfer in thick layers of SU-8 photoresist to create a metal master of microneedles. A elastomer mold [polydimethylsiloxane (PDMS)] is cast from the metal master, and polymeric microneedles are cast from the mold. The microneedles, about  $500\ \mu\text{m}$  in height, have a beveled tip to reduce the insertion force. Various polymers were investigated, including a biodegradable polymer, polyglycolide (PGA) incorporating model compounds to mimic controlled drug release. The polymer microneedles can be loaded with a drug or protein, which delivers the drug by diffusion or as the structures degrade. These microneedles successfully penetrated human epidermis without breaking. Depth profiling of the released model compounds showed successful penetration to  $200\ \mu\text{m}$ .

### III. DELIVERY OF DNA USING MICROSTRUCTURES

Several gene transfer techniques have been developed for the introduction of foreign genes into both plant and animal cells. One of the more commonly used methods is cell bombardment, in which small particles coated with genetic material are ballistically transported into target cells [26].

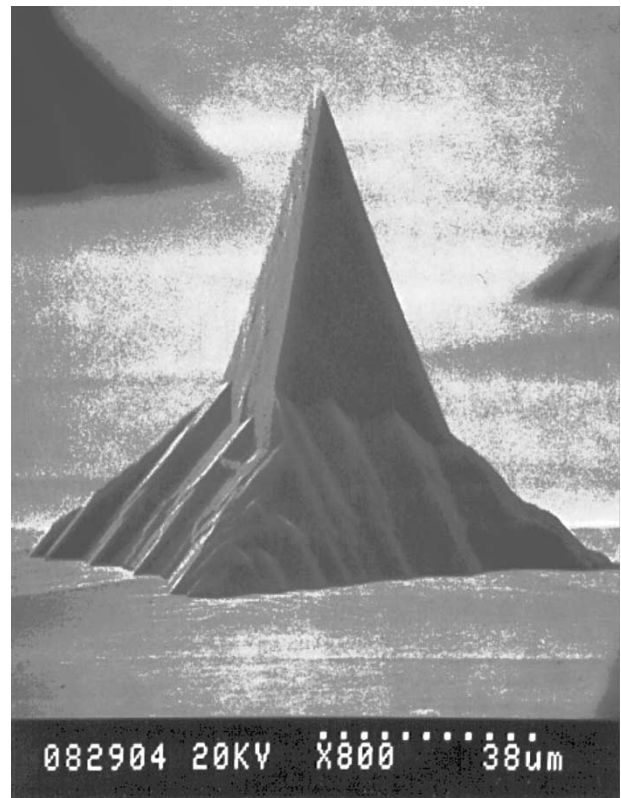
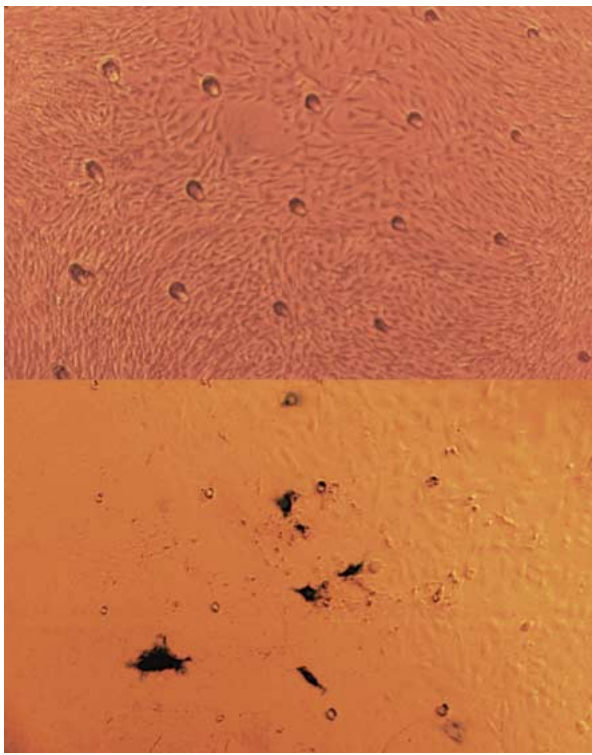


Fig. 13. Solid silicon microprobe for gene delivery [28].

Alternatively, electroporation techniques can be used; this involves the use of an electric field to transport the material across the cell wall [27]. An effective but laborious and time-consuming method needing highly skilled practitioners is direct microinjection. In this technique, a fine hypodermic needle is inserted into the target cell by direct manipulation under a microscope; the DNA is then directed through the needle lumen.

Another method is to use micromechanical piercing structures, as shown in Fig. 13. These structures, fabricated in dense arrays using bulk micromachining of silicon, are approximately  $80\ \mu\text{m}$  high topped by a wedge-shaped tip with a radius of curvature less than  $0.1\ \mu\text{m}$ . The facets of the microprobes are composed of fast-etching (411) planes, produced by convex-corner undercutting in an anisotropic etching solution of a square mask [28]. When the microprobes are coated with genes and pressed into cells or tissues, the sharp tips penetrate into the cells and effect the transport of genetic material, which is subsequently expressed in the target cells and their progeny. Successful expression of foreign genes using this technique has been demonstrated in the nematode *Caenorhabditis elegans* [29] and tobacco leaf cells [30].

Feldman *et al.* [31] have shown that microprobe-mediated gene transfection can also be performed in mammalian cells. In these experiments, smooth muscle cells from rat arteries were cultured. A solution containing DNA was centrifuged onto microprobe arrays and pressed into smooth muscle cell monolayer samples. Fig. 14 illustrates typical results. At the top is shown a control sample in which no DNA was applied to microprobe tips. The regular pattern of dots, spaced



**Fig. 14.** DNA transfection using microprobes [57]. Top: control sample. Bottom: blue staining of smooth muscle cell nuclei demonstrates successful transfection.

250  $\mu\text{m}$  apart, are depressions caused by the microprobes as they were pressed through the cultured cells. The bottom picture illustrates successful incorporation and expression of the  $\beta$ -galactosidase transgene in the smooth muscle cells, as evidenced by the blue stains. Note that the staining is not coincident with the location of probe tips, which means that either the DNA was transported laterally away from the tips or, more likely, the cells have migrated after transfection. This, coupled with the lack of any evidence of dead cells, indicates that microprobes do not cause catastrophic cell injury during the transfection process.

These experiments all made use of solid microprobes, where the structures lacked lumens. The material of interest was coated onto the probe surface by dipping or centrifuging, and the arrays pressed into the cells, culture, or tissue. It is also possible to use microneedle structures, with lumens, for this application. Chun *et al.* [32]–[33] have fabricated arrays of hollow microcapillaries for controlled injection of genetic material into cells. Their fabrication process (Fig. 15) uses deep reactive ion etching of a silicon substrate to create trenches (approximately 100  $\mu\text{m}$ ) which are thermally oxidized. The substrate is then bonded to a Pyrex glass plate which will later form the carrier for the array. The silicon is back etched in a tetramethylammonium hydroxide (TMAH) solution to expose the tips of the oxidized trenches. A short etch in buffered HF removes the exposed oxide, creating hollow cylinders of  $\text{SiO}_2$  encased in the silicon. Further etching in TMAH attacks the silicon but not the  $\text{SiO}_2$ , resulting in arrays of silicon dioxide microcapillaries extending below the remaining silicon

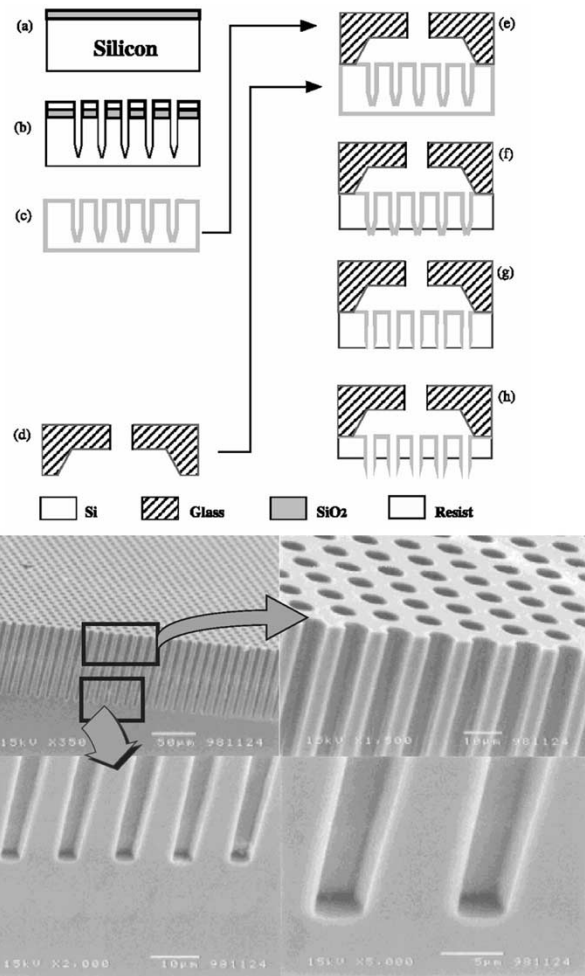


**Fig. 15.** Fabrication method for hollow microcapillary arrays for injection of genetic materials into cells developed by Chun *et al.* [33].

substrate (Fig. 16). These structures are approximately 5  $\mu\text{m}$  in diameter and 30  $\mu\text{m}$  long, with an array spacing of 20  $\mu\text{m}$ . Operation of the arrays was tested by injecting fluorescent dye under pressure into conglomerates of tobacco cells. Optical microscopy confirmed successful injection of liquid into the cells using these hollow microstructures.

Delivery of genes through the skin in a porcine model was demonstrated with a modified tattooing device by Eriksson *et al.* [34] The technique, dubbed “microseeding” by the authors, involves delivery of plasmid DNA solution to target cells by oscillating microneedles which penetrated approximately 2 mm below the surface of the skin. Successful transfection was observed and the animals were successfully protected from infection by the Swine influenza virus.

More recently, Mikszta *et al.* [35] used silicon microstructures to mechanically disrupt the top layer of skin (stratum corneum) and deliver DNA and vaccines to the epidermis. Fig. 17 shows the microstructures, which they call microenhancer arrays (MEAs), fabricated by isotropic chemical etching of silicon wafers. The structures are 50 to 200  $\mu\text{m}$  high, with a spacing of twice the height. The tops of the structures are not sharp points, but mesas with areas from 100 to 900  $\mu\text{m}^2$ . (These structures are similar to those

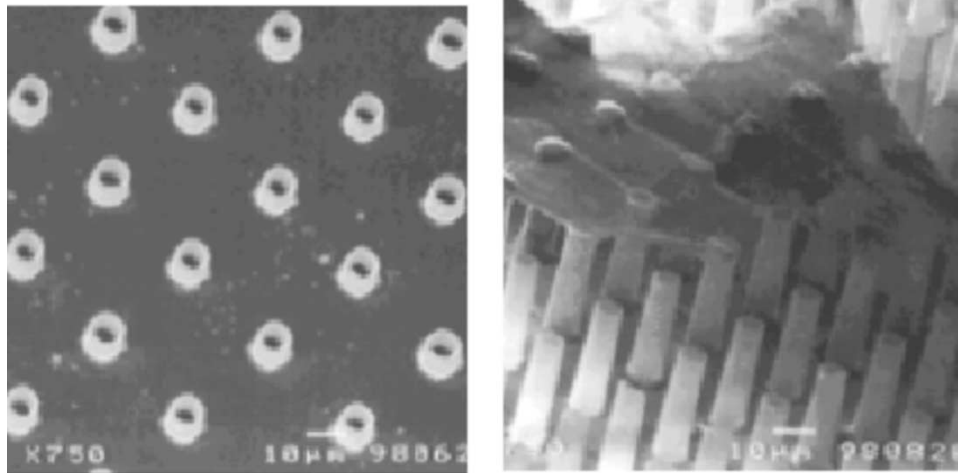


**Fig. 16.** Hollow microcapillary arrays of SiO<sub>2</sub> produced by the fabrication process of Chun *et al.* [33] (Fig. 15). The micrograph on the right shows a layer of tobacco cell conglomerates adhering to the microcapillaries after testing; no damage to the microstructures was noted.

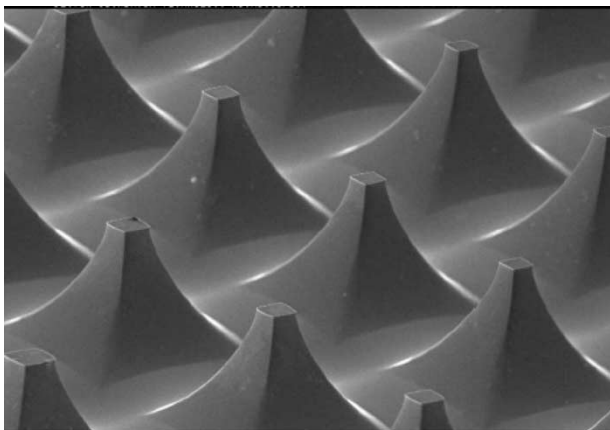


**Fig. 17.** Silicon microenhancer arrays for transdermal delivery of vaccines (from Mikszo *et al.* [35]).

fabricated by Ferrara *et al.* [36] for use as dermal abraders in plastic surgery.)

Initial experiments quantified the transepidermal water loss, a measure of the degree of mechanical disruption, of the MEAs using abrasive pads as a control. These pads are commonly used to prepare the surface of skin before attachment of electrocardiogram electrodes to improve conductivity. They found significant increases in the water loss when the MEA height exceeded 100  $\mu\text{m}$ . Treatment of the skin with 50- $\mu\text{m}$  MEAs and ECG preparation pads showed minimal or no increase in water loss. Only slight skin irritation was noted, which disappeared after 48 h, with no incidence of infections.

Gene transfer was demonstrated by coating MEAs with a solution containing naked plasmid DNA encoding firefly luciferase as a marker. Control experiments with topical application to the skin, intramuscular injection, and intradermal injection were also performed. The luciferase activity following delivery using MEAs increased from 1000- to 2800-fold compared to the topical control. This is greater than the gene expression obtained from both intramuscular injection (mean activity 460-fold above background) and

intradermal injection (mean activity 750-fold above background). It was necessary that the MEAs be scraped laterally across the skin; simply pressing the the MEAs vertically resulted in punctures but no significant gene transfer. Multiple passes of the MEAs resulted in increased gene expression.

The MEAs were also shown to enable genetic immunization via the skin. In this application, it is necessary that the vaccine penetrate through to the epidermis, as the stratum corneum is an effective barrier. Measurements of the immune response following MEA delivery indicated 100% seroconversion, compared to only 40% and 50% using vaccination via intramuscular and intradermal injection. Reproducibility of the immune response was found to be greater using MEA delivery.

These results show that microstructures are a promising method for delivery of genes and vaccines through the skin. MEA-based delivery induced stronger and less variable immune responses compared to both injections and other skin disruption techniques, and has minimal discomfort and skin irritation.

Microstructure arrays are attractive as a research tool for genetic engineering because they are relatively inexpensive, effective, and easy to use, especially in comparison with individual microinjection performed by a skilled operator. Most clinical efforts in gene therapy employ viral vectors to transport the DNA, but this has led to adverse reactions in some patients, including anaphylactic shock and even death. A natural extension is to use microstructures developed for research for *in vivo* therapeutic delivery. In the next section, we discuss the clinical application of microstructures for delivering therapeutic agents (drugs or genes) in the vascular system.

#### IV. DELIVERY OF ANTI-RESTENOSIS THERAPIES INTO CORONARY ARTERIES

Heart disease, evidenced by the progressive narrowing of coronary arteries by atherosclerotic plaque, continues to be a leading cause of death in the United States and worldwide. Commonly used transcatheter therapies for restoring

blood flow include balloon angioplasty (inflation of a balloon inside the artery, which compresses the plaque against the vessel wall), atherectomy (removal of the plaque with a cutting tool), and coronary stenting (placement of a metal cage-like device, the stent, as a mechanical scaffold). Despite the overall initial success of these procedures, approximately one-fifth to one-third of all patients will suffer restenosis (re-blockage) within six months of the initial procedure. Numerous pharmacological agents and genes have been shown to inhibit restenosis in animal models; however, many have failed in human trials. A chief difficulty is that local delivery methods relying on diffusion or pressure gradients are unable to transport therapeutic agents through the compressed layer of plaque, which can be up to 200  $\mu\text{m}$  thick.

Restenosis occurs not because of the factors leading to the original blockage, but in response to the angioplasty procedure. Balloon angioplasty is essentially a trauma-inducing event. The body responds to this trauma with a set of responses, including elastic recoil, smooth muscle cell migration and proliferation, associated extracellular matrix synthesis, vessel wall remodeling, and thrombus organization and incorporation [37]–[40]. The end result is the formation of a mass of material integrally coupled with the intimal wall. Elastic recoil of the vessel wall takes place after balloon deflation. Minutes following the injury, a thin layer of platelets and fibrin is deposited on the injured lumen. Within hours to days, inflammatory cells begin to infiltrate the site, and vascular smooth muscle cells begin to migrate toward the lumen. These smooth muscle cells then convert from their normal contractile phenotype to a synthetic phenotype in which they hypertrophy and begin to secrete extensive extracellular matrix, increasing the thickness of the intima [41]–[44]. These events are collectively termed “neointima” formation. During this time, the lumen surface is colonized by endothelial cells that slowly regain their normal barrier function and secretory functions in making tissue plasminogen activator and endothelial derived relaxation factor. The vessel media remodels to adjust for the restored lumen size.

If the vessel response to injury is excessive, most or all of the gain in lumen diameter produced by the initial interventional procedure may be lost to the healing process, with return of a severe stenosis and ischemic symptoms. During the 6-mo period when clinical restenosis occurs, different arteries appear to undergo varying degrees of proliferation and vessel remodeling, resulting in an observed patient-to-patient variation in the amount of late loss in lumen diameter. There tends to be a linear relationship between the late loss in lumen diameter caused by the healing response and the acute gain in lumen diameter caused by the intervention [45]. One consequence of this finding is that larger lumen diameters immediately after intervention translate into larger lumen diameters at the end of this 6-mo healing time. The acute gain in the lumen produced by the intervention is only partially lost during the repair process, resulting in a long-term net gain in lumen diameter.

Various mechanical devices have been developed in search for a way to reduce the incidence of restenosis. Of these mechanical devices, only intracoronary stenting has been shown to be successful (32% versus 42%).[46] The success of stenting has been attributed to the elimination of elastic recoil and fibrotic vessel contraction.

Further reduction of restenosis has been accomplished by delivering drug or gene therapy to the site of injury. Several attempts have been made to deliver anti-restenosis agents with various catheter-based systems locally in high concentrations to overcome the tolerated dose limitations of systemically administered therapeutics. These systems have been reviewed by Hofling and Huehns [48], and can be categorized as diffusion through close contact (i.e., hydrogel balloons, coated stents), pressure-driven diffusion (such as porous balloons and infusion sleeves), and mechanically assisted transport (needle catheters, iontophoretic balloons, cutting balloons). With these devices, successful delivery of pharmacological agents as well as genetic materials have been demonstrated in normal arteries [49]–[51].

Drug eluting stents have also been developed and are currently in clinical trials. These devices rely on drug diffusion from polymeric coatings to deliver therapeutics into the vessel wall. Diffusion as a drug distribution mechanism is, however, highly inefficient. Drugs tend to aggregate near the struts of the stent, leaving large voids between the struts with very low doses delivered into the vessel [52]. The resulting large local variation of drug concentration necessitates the use of drugs with very wide therapeutic windows; otherwise, the high levels of drug adjacent to the struts may be cytotoxic to vessel tissue. The efficacy of these devices depends critically on the tissue and cellular composition of the vessel wall and any pathologic indication that may be present. Both the internal elastic lamina (IEL) and atherosclerotic plaque serve as barriers to the transport of therapeutic agents, and available stents are not capable of penetrating these layers in a controlled fashion. In addition, the ultrastructure of vessel walls has been shown to have a significant impact on diffusive transmural drug delivery [53], resulting in efficacy variations across vessel types.

Despite these impediments, some drug eluting stents have shown significant reductions in restenosis rates [54]. To date, only a small subset of therapeutic agents tested have demonstrated clinical efficacy, these being low molecular weight lipophilic agents. The reliance on diffusion alone to transport therapeutics into the media obviates the use of larger molecules such as DNA or more hydrophilic compounds. For example, research by Feldman *et al.* [56] showed that delivery of reporter genes to atherosclerotic arteries was one-tenth as efficient as in normal arteries, owing to the presence of plaque, which acts as a diffusion barrier.

Because the etiology of restenosis involves many separate causes, with varying timelines, there is considerable interest in delivering more than one therapeutic agent. It would be especially useful to simultaneously deliver a drug (or drugs) which has short-term efficacy and a gene which transfects the cells in the vessel so they produce anti-proliferative agents over the long term. One approach is to engineer a

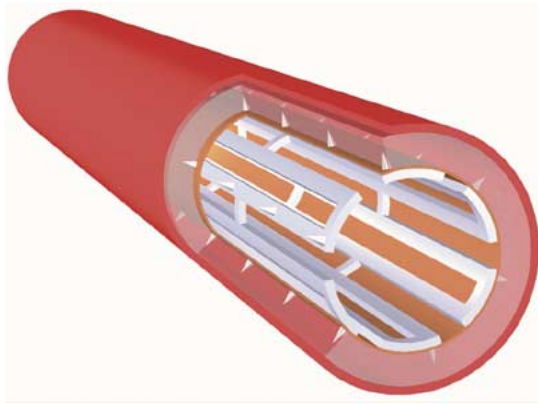


**Fig. 18.** Conceptual rendition of a translumina therapeutic delivery device. A stent is studded with microprobes capable of piercing through compressed arterial plaque and the internal elastic lamina to effect delivery of drugs or genes coating the device surface into the vessel media.

stent capable of overcoming the diffusion barriers and delivering therapeutic agents to reduce the incidence of restenosis. A conceptual diagram of the device is shown in Fig. 18 [57]. A metal stent is studded with microprobes capable of piercing atherosclerotic plaque and transecting the IEL. Therapeutic agents coating the stent can then be delivered into the vessel wall as the stent is deployed by an inflation balloon. Alternatively, a self-expanding device (typically fabricated from a shape memory alloy) could also serve as a microprobe-bearing platform.

Improved delivery results from two distinct mechanisms. The probes open up channels in the blocking layers (the compressed plaque and the IEL) both of which are diffusion barriers, especially for large molecules. Controlled incisions produced by the sharp microprobes, thus, increase the rate of diffusion. However, since the microprobe height can be controlled, it is possible to extend the incision height well into the vessel media, or even into the adventitia. This will facilitate diffusion of the therapeutic agent into the internal structure of the vessel, where lateral transport processes are considerably faster [53]. The more rapid transport would serve to equalize the distribution of the agent, producing a more uniform dose profile throughout the vessel. Conceivably, it is possible to deliver therapeutic agents into the vaso vasorum, the network of subvessels in the adventitia which supply the artery itself with oxygen; this would facilitate extremely fast intramural transport.

Because micromachined probes have been shown effective in transfecting mammalian smooth muscle cells, there are two issues to be considered for this device. The first issue is whether a microprobe is capable of piercing through an atherosclerotic vessel, and if so, what is the appropriate height, geometry, and pressure needed. Second, how can a three-dimensional structure like that shown in Fig. 18 be fabricated? Below we address these two points.

Preliminary work by Kneller *et al.* [58] has shown that microprobes are capable of transecting the wall of an atherosclerotic vessel. The scanning electron micrograph in Fig. 19 (top) illustrates in cross section a silicon microprobe,

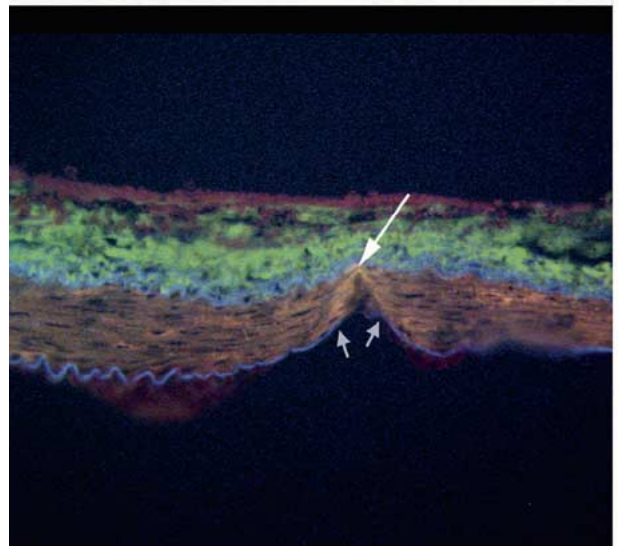
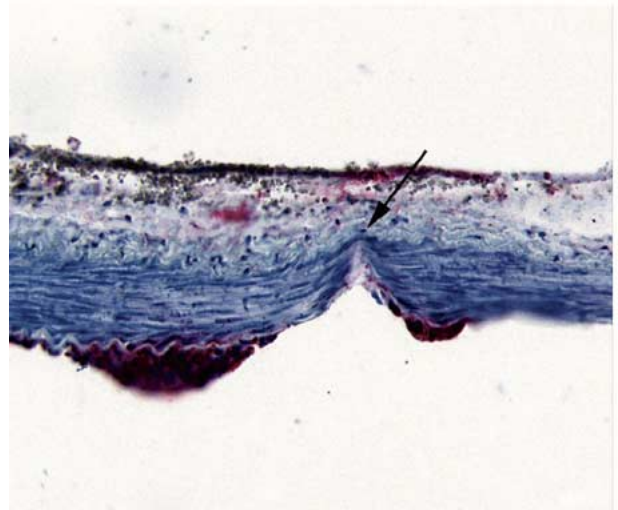
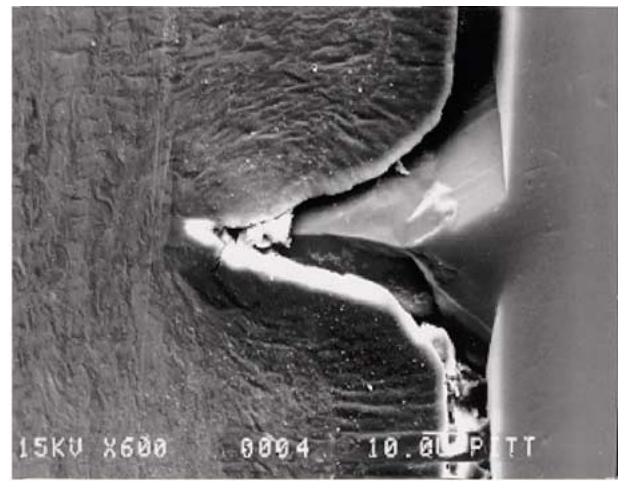


**Fig. 19.** Disruption of the internal elastic lamina by microprobes [57]–[58]. Top: insufficient height of the microprobes prevents penetration. Center and bottom: sufficiently tall microprobes are capable of piercing through atherosclerotic vessels.

approximately 80  $\mu\text{m}$  high, inserted into a filleted rabbit iliac artery (planar geometry). Although the microprobe is quite sharp, it has not penetrated through the IEL. Instead, the IEL has deformed around the microstructure.

Further experiments confirmed that microprobe height is the key variable. The center and lower parts of Fig. 19 show cross sections (bright field and fluorescent microscope images, respectively) of atherosclerotic vessels penetrated by 140- $\mu\text{m}$ -high microprobes at a pressure of 500-mm Hg. The plaque is visible in the center micrograph as large red areas. The fluorescence micrograph clearly shows the transection of the internal elastic lamina (dull blue). The area between the two small arrows indicates where the IEL is no longer continuous, having been disrupted by the microprobe. Other cross sections indicate that the success of transection depends strongly on the thickness of the plaque and the degree to which it covers the vessel intima.

Our objective is to extend these results to a clinical device precise enough to make controlled incisions into the vessel wall, accessing hidden tissue planes within which the etiology of restenosis resides, and to do so in a safe, efficacious manner with minimal risk of vessel perforation. A major constraint is that all microfabricated microneedle structures use techniques based on planar substrates, usually silicon. Coronary stents, in contrast, are fabricated from metal tubing (steel, titanium, cobalt chrome, nickel–titanium alloys) by mostly nonphotolithographic methods: laser machining, electrodischarge machining, electrochemical etching. These materials have a long history of use in medical implants, and are known to be largely biocompatible. Using lithographic-based technologies for fabricating a drug delivery stent is not desirable because of the challenges involved in having to develop new techniques for patterning and etching cylindrical metal tubing. The assembly of microfabricated silicon microneedles onto a stainless steel stent is also to be avoided, as this would excessively increase manufacturing complexity and cost.

Another complication relates to an important clinical issue. Modern stents are highly skeletal, with only a small fraction of the original tubing remaining after micromachining. Coronary stents are also quite small in diameter (“low profile” in medical jargon). These two features are necessary so that they can be maneuvered through the tortuous vasculature of the body and ultimately deployed in small-diameter vessels. Therefore, a clinically significant delivery device cannot have microprobes projecting from the stent surface until deployment, as this would unduly impede and complicate device delivery in the patient. (Fixed microprobes would likely tear at the intimal lining of the vessels all the way up to the point of deployment. Nor is it practical to sheath the fixed probes, as this limits the ability of the cardiologist to maneuver the device on its journey, and also constrains the minimum size vessel in which the device may be deployed.)

As such, the required device: 1) is low profile; 2) is stainless steel; 3) has microneedles which deploy toward the vessel wall only when the stent is in place and expanded. Given these constraints, a new approach is necessary. Ideally, it could be manufactured using existing stent machining technology (laser cutting of metal tubing), minimizing cleanroom lithographic processing on a cylindrical surface (lower cost, higher throughput), and has microneedles that

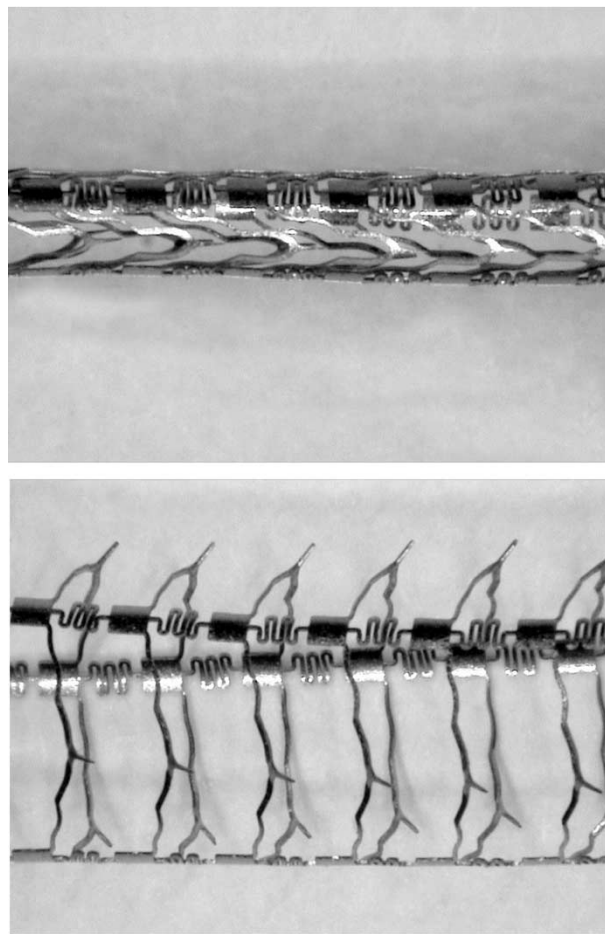


**Fig. 20.** Translaminar stent in its (a) undeployed and (b) deployed state.

only deploy when the device is expanded (safe delivery). (Microelectrodischarge machining techniques have been developed to fabricate nondelivery stents [59]; this approach permits rapid fabrication by using arrays of lithographically fabricated electrodes with simultaneous parallel discharges.)

The prototype of this translaminar stent, developed by the authors, is shown in Fig. 20 [60]. This device was laser machined and electropolished from a 1.5-mm (OD) tube of 316L stainless steel, with a wall thickness of 50  $\mu\text{m}$ . It is designed to be deployed in a vessel of 3.5-mm diameter by balloon expansion (Fig. 21). The device works on the principle of controlled balloon expansion—by allowing preferential expansion of the balloon into and under the barbed arm, the barb pivots upwards during inflation and presents the microneedle to the vessel wall. The mechanical deformation of the stent during deployment is, thus, used as a means of actuation, lifting the microneedles into position. By fabricating the microneedles “in plane” (i.e., the cylindrically shaped surface of the tubing) and deploying them “out of plane” toward the vessel wall only upon balloon inflation, it is possible to achieve great control in terms of needle dimensions and shape, without the limiting constraints of depth of focus when using a lithographic process. In addition to presenting a low profile, the translaminar stent is also flexible, as shown in Fig. 22. A primary concern

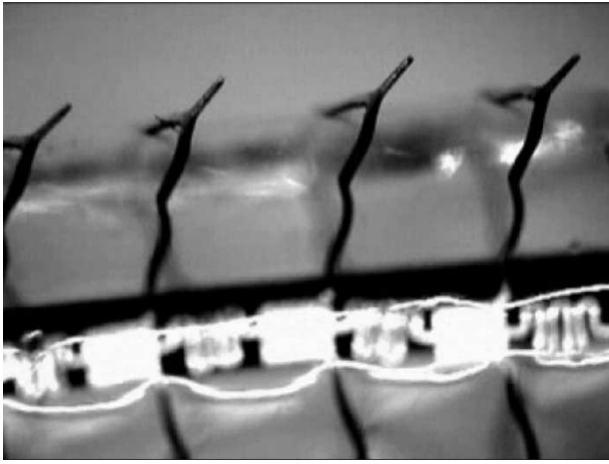


**Fig. 21.** Microneedles of the translamina stent are presented to the vessel wall upon balloon expansion.



**Fig. 22.** Flexibility of the translamina stent.

is the prevention of vessel perforation by the deployed microprobes. This issue has been addressed by restricting stent overexpansion, which is when perforations are likely to occur. The microneedles are arranged on circumferential rings that prevent the stent from expanding beyond its predesigned limit.

Controlled elution of the therapeutic agent from the surface of the stent through transections created by the microprobes is effected by creating a nanoporous layer over the outer surface of the device. We have used two methods of surface modification to create this nanoporous layer. One is to deposit a layer of a metal such as aluminum or titanium and subsequently anodize this layer to form an array of pores oriented normal to the metal surface. Pore density, aspect ratio, and diameter can be controlled by varying anodization parameters such as voltage, time, temperature, and electrolyte concentration. A second method is to deposit an alloy onto the laser cut, electropolished devices, and then subject the alloy to an electrochemical process that leaves behind a nanoporous gold film (Fig. 23). The high-quality, dense films of gold alloy exhibited good adhesion to the underlying metal. Processing of the films to create nanoporous structures further reduces film stress and improves adhesion.

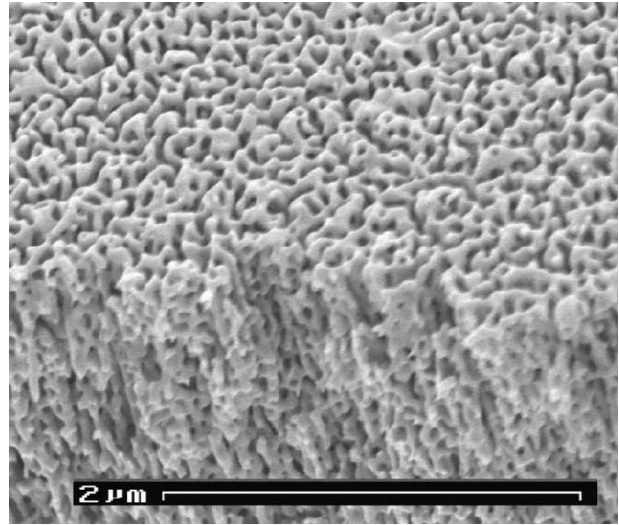


**Fig. 23.** Micrograph of nanoporous gold films used for therapeutic retention and elution.

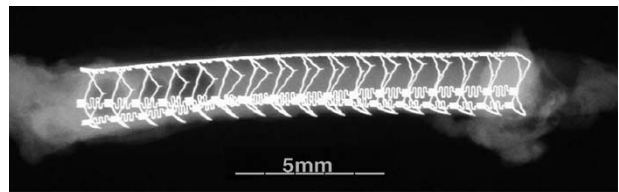


**Fig. 24.** X-ray showing successful deployment of a translamina stent in a rabbit femoral artery.

Therapeutic elution rates from the nanoporous coatings depends in part on pore size, pore depth, tortuosity, and areal density. These parameters can be controlled by varying the electrochemical processing conditions and the composition of deposited alloy.

The translamina stent has been successfully deployed *in vivo* in rabbit femoral arteries, as shown in Figs. 24 through 26 [61]. The microneedles are seen to make clean and precise incisions across the internal elastic lamina into the media. By modifying the device design, the microneedle penetration depth and deployment characteristics can be optimized for different vessels. Ongoing work will determine the long-term efficacy of this device, as well as the rate of delivery of therapeutic agents into the vessel wall.

## V. DISCUSSION

The use of needles to breach the skin in order to deliver therapeutics is not new: hypodermic needles have been in use since the mid-1800s. These devices were and are still typically utilized to deliver therapeutics systemically via the circulatory system. This is commonly done either by direct intravenous injection (for acute therapies, and requiring macroscopic needles) or by depositing a therapeutic dose subcutaneously, whereupon diffusion effects a more gradual and sustained release. The development of microneedles for transdermal delivery is aimed at achieving the latter therapy in a less traumatic fashion. In this application, the critical function of the microneedles is to breach the



**Fig. 25.** Cross-sectional micrograph of a translumina delivery device implanted in an artery showing penetration of microneedles into the vessel walls.

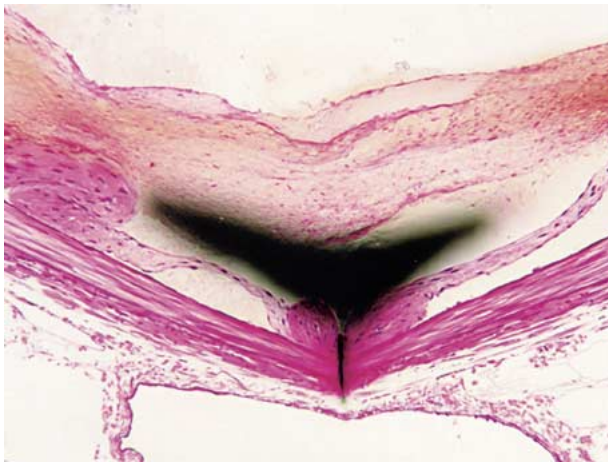


**Fig. 26.** Histology micrograph showing the precise incision of the media by a microneedle.

dermis in order to effect more efficient transport of therapeutics through the skin. The advent of microsystems and minimally invasive medical procedures has also allowed the development of intravascular delivery systems such as catheters and stents. Similar to the dermis, vascular walls [62]–[64] and certain pathologies present an effective barrier to molecular transport, which has led to the implementation of microstructures onto intravascular devices for transmural therapeutic delivery.

The clinical relevance of needle-based therapeutic delivery systems lies in their ability to physically localize delivery (to specific locations and/or tissues) and to effect transport across pathophysiologic barriers. As previously noted, skin provides an effective barrier to drug diffusion, as do the elastic laminae of blood vessel walls. Pathologies such as atherosclerotic plaques in coronary arteries also present a relatively impermeable barrier to drugs and genes.

While these diffusion barriers play an important role in drug transport, the mechanical delivery of therapeutics across these barriers does not, in itself, ensure clinical efficacy. In

addition to diffusive transport, many other factors affect the distribution of the therapeutic agent [65], [66]. The pharmacokinetics of the therapeutic agents play a significant part in the success or failure of a therapy. Factors such as nonspecific tissue binding can affect drug diffusion, resulting in drug segregation and uneven tissue concentrations. Hydrophilic drugs delivered on stents have been shown to aggregate near stent struts, while hydrophobic drugs diffuse more evenly into vessel walls [52]. Similarly, the circulatory system, while useful as a distribution mechanism for systemic therapies, can be detrimental to local therapies by eliminating therapeutics from target tissues. Local tissue ultrastructure and variations in diffusion constants within tissues can form virtual conduits which can rapidly eliminate drugs from one tissue plane while concentrating it in another. Pharmacologic deficiencies can also arise if the drug rapidly degrades or is eliminated by excretion.

As such, while microsystems can assist in drug delivery, clearly these devices cannot by themselves address all the issues associated with developing a clinically successful therapy. The engineering of these devices must be tailored to address the specific therapeutic to be delivered, as well as the local pathophysiology of the target delivery site. This presents significant opportunities for using the precision afforded by microfabrication to create microfabricated delivery systems that can locally target specific tissues within a patient with micrometer-level accuracy, breaching pathologic and physiologic barriers where necessary to effect clinically relevant doses of therapeutic agents.

## VI. SUMMARY

Microneedles and other structures can be fabricated using techniques traditionally employed in the manufacture of integrated circuits. These structures are useful for introducing therapeutic agents into tissues and cells. Microstructures for delivery through the skin greatly reduce the pain associated with drug injection, and are, thus, especially useful for patients with chronic conditions requiring frequent injections. Fluid delivery microstructures can be integrated with microelectrodes for *in situ* monitoring of tissue response. Microfabricated structures are also useful in delivering genes in both plants and animals, and are less costly than competing methods. Microfabricated delivery devices hold great promise for local delivery of drugs and genes where systemic administration presents serious safety concerns. Microsystems technology has the potential to radically improve the range of applications for local delivery by the creation of new delivery platforms, which will in turn enable the development of new therapies. One such device is the translumina stent which deploys microprobes capable of delivering drugs or genes. Preliminary testing of this device has demonstrated successful deployment and incision of the vessel wall in rabbit femoral arteries. Microfabricated devices could also be useful in studying, *in vivo*, local microscale transport phenomena, which are necessary to understand the pharmacokinetics of local delivery.

## ACKNOWLEDGMENT

The authors would like to thank M. Feldman, R. Hanumanthai, D. Patel, K. Looi, L. Weiss, M. Wholey, C. Wu, J. Kneller, K. Rebello, M. Prausnitz, G. Stemme, S. Roy, B. Frazier, and M. Allen for many stimulating discussions.

## REFERENCES

- [1] D. V. McAllister, M. G. Allen, and M. R. Prausnitz, "Microfabricated microneedles for gene and drug delivery," *Annu. Rev. Biomed. Eng.*, vol. 2, pp. 289–313, 2000.
- [2] J. D. Brazzle, I. Papautsky, and A. B. Frazier, "Micromachined needle arrays for drug delivery or fluid extraction," *IEEE Eng. Med. Biol. Mag.*, vol. 18, pp. 53–58, Nov.–Dec. 1999.
- [3] J. D. Brazzle, I. Papautsky, and A. B. Frazier, "Fluid-coupled hollow metallic micromachined needle arrays," in *Proc. SPIE, Microfluidic Devices and Systems*, vol. 3515, 1998, pp. 116–124.
- [4] J. D. Brazzle, S. Mohanty, and A. B. Frazier, "Hollow metallic micromachined needles with multiple output ports," in *Proc. SPIE, Microfluidic Devices and Systems II*, vol. 3877, 1999, pp. 257–266.
- [5] I. Papautsky, J. Brazzle, H. Swerdlow, R. Weiss, and A. B. Frazier, "Micromachined pipette arrays," *IEEE Trans. Biomed. Eng.*, vol. 47, pp. 812–819, June 2000.
- [6] S. Chandrasekaran and A. B. Frazier, "Mechanical characterization of surface micromachined hollow metallic microneedles," in *IEEE EMBS Special Topic Conf. Microtechnologies Medicine and Biology*, 2002, pp. 94–98.
- [7] S. Chandrasekaran and A. B. Frazier, "Characterization of surface micromachined hollow metallic microneedles," in *Proc. 16th Annu. Int. Conf. Micro Electro Mechanical Systems*, 2003, pp. 363–366.
- [8] L. Lin and A. P. Pisano, "Silicon-processed microneedles," *J. Microelectromech. Syst.*, vol. 8, no. 1, pp. 78–84, Mar. 1999.
- [9] J. Chen, K. D. Wise, J. F. Hetke, and S. C. Bledsoe Jr., "A multi-channel neural probe for selective chemical delivery at the cellular level," *IEEE Trans. Biomed. Eng.*, vol. 44, pp. 760–769, Aug. 1997.
- [10] N. H. Talbot and A. P. Pisano, "Polymolding: Two wafer polysilicon micromolding of closed-flow passages for microneedles and microfluidic devices," in *Tech. Dig. Solid-State Sensor and Actuator Workshop*, 1998, pp. 265–268.
- [11] J. D. Zahn, N. H. Talbot, D. Liepmann, and A. P. Pisano, "Microfabricated polysilicon microneedles for minimally invasive biomedical devices," *Biomed. Microdev.*, vol. 2, no. 4, pp. 295–303, 2000.
- [12] J. D. Zahn, D. Trebotich, and D. Liepmann, "Microfabricated microdialysis microneedles for continuous medical monitoring," in *Proc. 1st Annu. Int. IEEE-EMBS Special Topic Conf. Microtechnologies Medicine and Biology*, 2000, pp. 375–380.
- [13] J. D. Zahn, A. A. Deshmukh, A. P. Pisano, and D. Liepmann, "Continuous on-chip micropumping through a microneedle," in *Tech. Dig. 14th IEEE Int. Conf. Micro Electro Mechanical Systems*, 2001, pp. 503–506.
- [14] J. D. Zahn, A. A. Deshmukh, A. P. Papavasiliou, A. P. Pisano, and D. Liepmann, "An integrated microfluidic device for the continuous sampling and analysis of biological fluids," presented at the 2001 ASME Int. Mechanical Engineering Congress and Exposition, New York.
- [15] K. Oka, S. Aoyagi, Y. Arai, Y. Isono, G. Hashiguchi, and H. Fujita, "Fabrication of a micro needle for a trace blood test," *Sens. Actuators A, Phys.*, vol. 97–98, pp. 478–485, 2002.
- [16] B. Stoerber and D. Liepmann, "Two-dimensional arrays of out-of-plane needles," in *Proc. ASME Int. Mechanical Engineering Congr. and Exposition*, 2000, pp. 355–359.
- [17] B. Stoerber and D. Liepmann, "Fluid injection through out-of-plane microneedles," in *Proc. 1st Annu. Int. IEEE-EMBS Special Topic Conf. Microtechnologies Medicine and Biology*, 2000, pp. 224–228.
- [18] B. Stoerber and D. Liepmann, "Design, fabrication and testing of a MEMS syringe," presented at the Solid-State Sensor, Actuator and Microsystems Workshop, Hilton Head, SC, 2002.
- [19] S. Henry, D. V. McAllister, M. G. Allen, and M. R. Prausnitz, "Micromachined needles for the transdermal delivery of drugs," in *Proc. IEEE 11th Annu. Int. Workshop Micro Electro Mechanical Systems*, 1998, pp. 494–498.
- [20] S. Henry, D. V. McAllister, M. G. Allen, and M. R. Prausnitz, "Microfabricated microneedles: A novel approach to transdermal drug delivery," *J. Pharm. Sci.*, vol. 87, no. 8, pp. 922–925, 1998.
- [21] H. Jansen, M. de Boer, B. Otter, and M. Elwenspoek, "The black silicon method IV: The fabrication of three dimensional structures in silicon with high aspect ratios for scanning probe microscopy and other applications," in *Proc. 8th Int. Workshop Micro Electro Mechanical Systems*, 1995, pp. 88–93.
- [22] P. Griss and G. Stemme, "Novel, side opened out-of-plane microneedles for microfluidic transdermal interfacing," in *Tech. Dig. 15th IEEE Int. Conf. Micro Electro Mechanical Systems*, 2002, pp. 467–470.
- [23] P. Griss and G. Stemme, "Novel, Side-opened out-of-plane microneedles for microfluidic transdermal liquid transfer," *J. Microelectromech. Syst.*, vol. 12, no. 3, pp. 296–301, 2003.
- [24] J. G. E. Gardeniers, J. W. Berenschot, M. J. de Boer, Y. Yeshurun, M. Hefetz, R. van't Oever, and A. van den Berg, "Silicon micromachined hollow microneedles for transdermal liquid transfer," in *Proc. IEEE Conf. MEMS*, 2002, p. 141.
- [25] J.-H. Park, S. Davis, Y.-K. Yoon, M. R. Prausnitz, and M. G. Allen, "Micromachined biodegradable microstructures," *Proc. IEEE Conf. MEMS*, pp. 371–374, 2003.
- [26] T. M. Klein, E. D. Wolf, R. Wu, and J. C. Sanford, "High velocity microprojectile for delivering nucleic acids into living cells," *Nature*, vol. 327, pp. 70–73, 1987.
- [27] H. Potter, L. Weir, and P. Leder, "Enhancer-dependent expression of human k immunoglobulin genes introduced into mouse pre-B lymphocytes by electroporation," *Proc. Nat. Acad. Sci.*, vol. 81, pp. 7161–7165, 1984.
- [28] R. Dizon, H. Han, A. G. Russell, and M. L. Reed, "An ion milling pattern transfer technique for fabrication of three-dimensional micro-mechanical structures," *J. Microelectromech. Syst.*, vol. 2, no. 4, pp. 151–159, 1993.
- [29] S. Hashmi, P. Ling, G. Hashmi, M. L. Reed, R. Gaugler, and W. Trimmer, "Genetic transformation of nematodes using arrays of micro-mechanical piercing structures," *BioTechniques*, vol. 19, no. 5, pp. 766–770, 1995.
- [30] W. Trimmer, P. Ling, C.-K. Chin, P. Orton, R. Gaugler, S. Hashmi, G. Hashmi, B. Brunett, and M. L. Reed, "Injection of DNA into plant and animal tissues with micro-mechanical piercing structures," in *Proc. 8th Int. Workshop Micro Electro Mechanical Systems*, 1995, pp. 111–115.
- [31] M. D. Feldman, B. Sun, B. J. Koci, C. C. Wu, J. R. Kneller, H. S. Borovetz, S. Watkins, A. Nadeem, L. E. Weiss, M. L. Reed, A. J. C. Smith, and W. Rosenblum, "Stent-based gene therapy," *J. Long-Term Effects Med. Implants*, vol. 10, no. 1–2, pp. 47–68, 2000.
- [32] K. Chun, G. Hashiguchi, H. Toshiyoshi, H. Fujita, Y. Kikuchi, J. Ishikawa, Y. Murakami, and E. Tamiya, "An array of hollow microcapillaries for the controlled injection of genetic materials into animal/plant cells," in *Tech. Dig. 12th IEEE Int. Conf. Micro Electro Mechanical Systems*, 1999, pp. 406–411.
- [33] K. Chun, G. Hashiguchi, H. Toshiyoshi, and H. Fujita, "Fabrication of array of hollow microcapillaries used for injection of genetic materials into animal/plant cells," *Jpn. J. Appl. Phys. 2, Lett.*, vol. 38, no. 3A, pp. L279–L281, Mar. 1, 1999.
- [34] E. Eriksson, F. Yao, T. Svensjo, T. Winkler, J. Slama, M. D. Macklin, C. Andree, M. McGregor, V. Hinshaw, and W. F. Swain, "In vivo gene transfer to skin and wound by microseeding," *J. Surg. Res.*, vol. 78, pp. 85–91, 1998.
- [35] J. A. Mikszta, J. B. Alarcon, J. M. Brittingham, D. E. Sutter, R. J. Pettis, and N. G. Harvey, "Improved genetic immunization via micro-mechanical disruption of skin-barrier function and targeted epidermal delivery," *Nature Med.*, vol. 8, no. 4, pp. 415–419, 2002.
- [36] L. A. Ferrara, A. J. Fleischman, E. C. Benzel, and S. Roy, "Micromachined dermabraders for plastic surgical applications," in *Tech. Dig. 15th IEEE Int. Conf. Micro Electro Mechanical Systems*, 2002, pp. 44–47.
- [37] J. B. Simpson, M. R. Selmon, G. C. Robertson, P. R. Cipriano, W. G. Hayden, D. E. Johnson, and J. E. Fogarty, "Transluminal atherectomy for occlusive peripheral vascular disease," *Amer. J. Cardiol.*, vol. 61, p. 96G, 1988.
- [38] R. D. Safian, C. L. Grines, M. A. May, A. Lichtenberg, N. Juran, T. L. Schreiber, G. Pavlikdes, T. B. Meany, V. Savas, and W. W. O'Neill, "Clinical and angiographic results of transluminal extraction coronary atherectomy in saphenous vein bypass grafts," *Circulation*, vol. 89, p. 302, 1994.
- [39] S. S. Ahn, D. Auth, D. R. Marcus, and W. S. Moore, "Removal of focal atheromatous lesions by angioscopically guided high-speed rotary atherectomy," *J. Vasc. Surg.*, vol. 7, p. 292, 1988.
- [40] J. L. Fourier, M. E. Bertrand, D. C. Auth, J. M. Lablanche, A. Gommeaux, and J. M. Brunetraud, "Percutaneous coronary rotational atherectomy in humans: Preliminary report," *J. Amer. Coll. Cardiol.*, vol. 14, pp. 1278–1282, 1989.

- [41] J. H. Ip, V. Fuster, D. Israel, L. Badimon, J. Badimon, and J. H. Chesebro, "The role of platelets, thrombin and hyperplasia in restenosis after coronary angioplasty," *J. Amer. Coll. Cardiol.*, vol. 17, pp. 77B-88B, 1991.
- [42] J. Forrester, M. Fishbein, and R. Helfant, "A paradigm of restenosis based on cell biology: Clues for the development of new preventive therapies," *J. Amer. Coll. Cardiol.*, vol. 17, pp. 758-769, 1991.
- [43] W. Casscells, "Migration of smooth muscle and endothelial cells: Critical events in restenosis," *Circulation*, vol. 86, pp. 723-729, 1992.
- [44] J. T. Willerson, S. K. Yao, J. McNatt, C. R. Benedict, H. V. Anderson, P. Golino, S. S. Murphree, and L. M. Buja, "Frequency and severity of cyclic flow alterations and platelet aggregation predict the severity of neointimal proliferation following experimental coronary stenosis and endothelial injury," *Proc. Nat. Acad. Sci.*, vol. 88, pp. 10 624-10 628, 1991.
- [45] D. S. Baim, "Coronary angioplasty," in *Cardiac Catheterization, Angiography, and Intervention*, 5th ed, D. S. Baim and W. Grossman, Eds. Baltimore, MD: Williams & Wilkins, ch. 27, p. 558.
- [46] D. L. Fischman, M. B. Leon, and D. S. Baim, "A randomized comparison of coronary stent placement and balloon angioplasty in the treatment of coronary artery disease," *New Engl. J. Med.*, vol. 331, no. 8, pp. 496-501, 1994.
- [47] J.P. Carrozza, Jr. and D. S. Baim, "Coronary stenting," in *Cardiac Catheterization, Angiography, and Intervention*, 5th ed, D. S. Baim and W. Grossman, Eds. Baltimore, MD: Williams & Wilkins, ch. 29, p. 618.
- [48] B. Hofling and T. Y. Huehns, "Intravascular local drug delivery after angioplasty," *Eur. Heart J.*, vol. 16, pp. 437-440, 1995.
- [49] R. Riessen, H. Rahimizadeh, E. Blessing, S. Takeshita, J. J. Barry, and J. M. Isner, "Arterial gene transfer using pure DNA applied directly to a hydrogel-coated angioplasty balloon," *Human Gene Therapy*, vol. 4, no. 6, pp. 749-758, 1993.
- [50] R. Riessen and J. M. Isner, "Prospects for site-specific delivery of pharmacologic and molecular therapies," *J. Amer. Coll. Cardiol.*, vol. 23, no. 5, pp. 1234-1244, 1994.
- [51] C. Unterberg, A. B. Buchwald, P. Barath, T. Schmidt, H. Kreuzer, and V. Wiegand, "Cutting balloon coronary angioplasty-initial clinical experience," *Clin. Cardiol.*, vol. 16, no. 9, pp. 660-664, 1993.
- [52] C.-W. Hwang, D. Wu, and E. R. Edelman, "Physiological transport forces govern drug distribution for stent-based delivery," *Circulation*, vol. 104, pp. 600-605, 2001.
- [53] C.-W. Hwang and E. R. Edelman, "Arterial ultrastructure influences transport of locally delivered drugs," *Circulation Res.*, vol. 90, pp. 826-832, 2002.
- [54] J. E. Sousa, M. A. Costa, A. C. Abizaid, B. J. Rensing, A. S. Abizaid, L. F. Tanajura, K. Kozuma, G. van Lengenhove, A. G. M. R. Sousa, R. Falotico, J. Jaeger, J. J. Popma, and P. Serruys, "Sustained suppression of neointimal proliferation by sirolimus-eluting stents: one-year angiographic and intravascular ultrasound follow-up," *Circulation*, vol. 104, pp. 2007-2011, 2001.
- [55] J. R. Kneller, "Penetrating through atherosclerotic plaque into rabbit arteries with microfabricated probes," M.S. thesis, University of Pittsburgh, Pittsburgh, PA, 1997.
- [56] L. J. Feldman, P. G. Steg, L. P. Zheng, D. Chen, M. Kearney, S. E. McGarr, J. J. Barry, J. F. Dedieu, M. Perricaudet, and J. M. Isner, "Low-efficiency of percutaneous adenovirus-mediated arterial gene transfer in the atherosclerotic rabbit," *J. Clin. Investigat.*, vol. 95, pp. 2662-2671, 1995.
- [57] M. L. Reed, C. C. Wu, J. R. Kneller, S. Watkins, D. A. Vorp, A. Nadeem, L. E. Weiss, K. Rebello, M. Mescher, A. J. C. Smith, W. Rosenblum, and M. D. Feldman, "Micromechanical devices for intravascular drug delivery," *J. Pharm. Sci.*, vol. 87, no. 11, pp. 1387-1394, 1998.
- [58] J. R. Kneller, C. C. Wu, D. A. Vorp, M. L. Reed, L. E. Weiss, H. S. Borovetz, S. Watkins, and M. D. Feldman, "The use of microfabricated probes to penetrate the internal elastic lamina and intimal hyperplasia," *J. Cardiovasc. Diagnosis Procedures*, vol. 16, no. 2, pp. 37-50, 1999.
- [59] K. Takahata and Y. B. Gianchandani, "Coronary artery stents microfabricated from planar metal foil: Design, fabrication, and mechanical testing," in *Proc. 16th IEEE Int. Conf. Micro Electro Mechanical Systems*, 2003, pp. 462-465.
- [60] W.-K. Lye and M. L. Reed, "Stainless steel microsystems for intravascular therapeutic delivery," presented at the Spring 2003 Meeting Materials Research Society, San Francisco, CA.
- [61] M. Feldman, Unpublished data, Health Sciences Center, University of Texas, San Antonio, .
- [62] C. P. Winlove, K. H. Parker, and A. R. Ewins, "The uptake of ions and neutral solutes by the artery and by artery wall preparations," *Connect. Tissue Res.*, vol. 18, pp. 83-93, 1998.
- [63] M. S. Penn, G. M. Saidel, and G. M. Chisolm, "Relative significance of endothelium and internal elastic lamina in regulating the entry of macromolecules into arteries in vivo," *Circulation Res.*, vol. 74, pp. 74-82, 1994.
- [64] M. S. Penn, M. R. Koelle, S. M. Schwartz, and G. M. Chisolm, "Visualization and quantification of transmural concentration profiles of macromolecules across the arterial wall," *Circulation Res.*, vol. 67, pp. 11-22, 1990.
- [65] P. Opanasopit, M. Nishikawa, and M. Hashida, "Factors affecting drug and gene delivery: effects of interaction with blood components," *Crit. Rev. Therapeutic Drug Carrier Syst.*, vol. 19, no. 3, pp. 191-233, 2002.
- [66] J. E. Talmadge, "The pharmaceuticals and delivery of therapeutic polypeptides and proteins," *Adv. Drug Delivery Rev.*, vol. 10, pp. 247-299, 1993.



**Michael L. Reed** (Senior Member, IEEE) received the B.S. and M.Eng. degrees in electrical engineering from Rensselaer Polytechnic Institute, Troy, NY, in 1979 and 1980, respectively, and the Ph.D. degree in electrical engineering from Stanford University, Stanford, CA.

He has held appointments at Hewlett-Packard Laboratories, Carnegie-Mellon University, University of Twente, ETH Zürich, and the Albert Ludwigs Universität, Freiburg. He is currently Professor of Electrical Engineering and

Biomedical Engineering at the University of Virginia, Charlottesville. With R. Rohrer, he is the author of *Applied Introductory Circuit Analysis for Electrical and Computer Engineers* (Englewood Cliffs, NJ: Prentice-Hall, 1998) as well as numerous research publications. He is an Editor of the journal *Sensors and Materials*. He currently holds nine issued and nine pending patents related to microsystems technology and microfabricated medical devices. His research interests center on microfabrication technology and microsystems applications.

Dr. Reed is a Fellow of the Institute of Physics. He was the Technical Chairman of the 1995 IEEE International Workshop on MEMS, and the General Chairman of the 1996 Workshop. He also organized the 1996 Materials Research Society Symposium on Materials in Microsystems. He is a recipient of the Hertz Foundation Prize and a Presidential Young Investigator Award.



**Whye-Kei Lye** (Member, IEEE) received the B.Sc. degree in physics from the California Institute of Technology, Pasadena, in 1993 and the M.Sc., M.Phil., and Ph.D. degrees in applied physics from Yale University, New Haven, CT, in 1994, 1996, and 1998, respectively.

As a graduate student, he interned at Texas Instruments, Dallas, TX, where he worked on advanced memory devices. He is currently a Research Scientist in the Department of Electrical and Computer Engineering, University of Virginia, Charlottesville. His graduate research focused on the study of MOS tunnel junctions using inelastic electron tunneling spectroscopy. He is currently working on developing microsystems for biomedical applications, and has four pending patents in this field.